Chapter 5

Observational Data for Black Carbon

5.1 Summary of Key Messages

- Estimates of BC are made with a variety of instrumentation and measurement techniques. Most ground level estimates of BC are reported as mass concentrations based on thermal-optical (EC) and filter-based optical (BC) techniques. BC and EC values from these measurement methods are highly correlated, although the method-defined values may differ by as much as a factor of two; however, consistent measurements in long-term monitoring networks are sufficient to detect trends that correlate with emissions reductions. Published studies show that BC:EC ratios derived by commercial instrumentation are generally within 30%.

- The United States has recently standardized BC measurements for its major routine speciation monitoring networks. Additional research is needed to further standardize ambient and emissions measurement methods and to develop factors that harmonize existing measurements produced from different sampling and analytical techniques. It is also recommended that light absorption be reported in the original units of absorption along with any mass absorption coefficients or conversion factors used to convert absorption to BC mass concentration.

- Ground-level BC measurements across the globe indicate estimated concentrations ranging from < 0.1 μg/m^3 in remote locations to ~15 μg/m^3 in urban centers. Although monitor locations are sparse globally, available observations suggest ambient levels in China are almost 10 times higher in urban and rural areas than those in North America or Europe. A comparison of urban concentrations to corresponding regional background levels reveals an urban increment of up to 2 μg/m^3 in North America and Europe compared to an urban increment of ~6-11 μg/m^3 in China.

- In the United States, BC comprises ~5-10% of average urban $PM_{2.5}$ mass.

- Long-term records of historical BC concentrations, derived from sediments or ice cores, valuably supplement available ambient data.

  - Long term trends in estimated ambient concentrations derived from BC in sediments of the New York Adirondacks and Lake Michigan show recent maximum concentrations occurred in the early- to mid-1900s and it appears concentrations have since decreased, which is attributed to decreased U.S. fossil fuel BC emissions.

  - Ice core measurements in Greenland reveal a similar maximum BC level in the early 1900s related to industrial emissions, but also show that biomass burning emissions contribute significantly to deposited BC in the Arctic.

  - Globally, Northern Hemispheric ice core BC trends vary with location; some ice cores have BC values increasing to present-day, while other areas show maximum levels reached earlier in the 1900s.

- Over the past two decades when U.S. ground-level ambient BC measurements are available, ambient BC concentrations have declined substantially, most likely due to reductions in mobile source emissions and other controls on direct $PM_{2.5}$ emissions. Since 2007, the decline may be due in part to recession-related decreases in vehicular travel and industrial output. The ambient concentration declines appear to be stronger in urban areas and may in fact be larger than the estimated average reductions in total BC and direct $PM_{2.5}$ emissions in the United States.

- Estimates of the total atmospheric column using remote sensing qualitatively show similar spatial variability in absorbing aerosol levels across the globe to ground level measurements. Remote sensing measurements that utilize multiple wavelengths also show that the absorbing particle mixture varies globally among areas dominated by urban-industrial sources, biomass burning, and wind-blown dust.

5.2 BC and Other Light-Absorbing Carbon: Measurement Methods

Current measurement techniques generally estimate BC on the basis of light absorption characteristics or by thermally isolating a specific carbon fraction. The techniques used currently to estimate BC mass concentrations are summarized in Table 5-1. These two general categories of BC measurement techniques can be viewed as different indicators of the chemical and physical properties of BC.[1] This is discussed further in the text box, "Measurement Approaches for BC." The two most common BC measurement techniques are thermal-optical and filter-based light absorption as denoted in the table below.

Table 5-1. Description of BC Measurement Techniques.

Method Type	Method Description	Prevalence of Use
Light absorption/optical	*Filter-based:* Light absorption by particles is measured through a filter loaded with particles; BC is quantified using factors that relate light absorption to a mass concentration.	High
	Photoacoustic: Light absorption by particles is measured by heated particles transferring energy to the surrounding air and generating sound waves; BC is quantified using factors that relate light absorption to a mass concentration.	Low
	Incandescence: Incandescent (glowing) particle mass is measured; BC is quantified by calibrating the incandescent signal to laboratory-generated soot.	Low
Isolation of specific carbon fraction	*Thermal-Optical:* BC is measured as the carbon fraction that resists removal through heating to high temperatures and has a laser correction for carbon that chars during the analysis procedure; BC is quantified as the amount of carbon mass evolved during heating.	High
	Thermal: BC is measured as the carbon fraction that resists removal through heating to high temperatures; BC is quantified as the amount of carbon mass evolved during heating.	Low

Thermal-optical measurements involve exposing a particle-laden filter to a series of heating steps. These measurements involve a multi-step temperature program to evolve OC in pure helium and EC in a helium/oxygen atmosphere with an optical (transmittance or reflectance) correction for pyrolysis or the charring of organic material during analysis. Despite the seeming simplicity of thermally separating particulate carbon into two fractions, there is considerable uncertainty in assigning carbon mass to either OC or EC fractions. For example, charring of particles during the thermal analysis has produced erroneous OC and EC assignments (Cadle et al., 1980; Huntzicker et al., 1982; Yu et al., 2002b). In addition, there are several different commonly used temperature protocols that cause variation in the OC and EC assignments. Watson et al. (2005) and Chow et al. (2006) provide a detailed summary of the variety of methods used that demonstrates the wide range of thermal analysis protocols in use. The two thermal-optical methods that are predominantly used in monitoring networks in the United States are the thermal-optical transmittance (TOT) and thermal-optical reflectance (TOR) methods (Chow et al., 1993; Chow et al., 2007; Peterson and Richards, 2002). The TOT method differs from the TOR method in the thermal combustion program used and the method of correcting for char (transmittance versus reflectance). Long-standing reliance on the thermal optical methods has resulted in an extensive observational record based on OC/EC splits, and the frequent use of EC as an estimate of BC.

While EC is directly quantified as the mass of carbon atoms that evolve during a thermal or thermal-optical analysis, optical techniques observe the light-absorbing properties of the particles to estimate BC. Filter-based, optical instruments are relatively low cost, readily available, and simple to operate, and thus are frequently field deployed

[1] In current practice, measurements produced from light absorption/optical methods are expressed as BC while those produced from thermal-optical or thermal methods are referred to as EC. To simplify the discussion, this differentiation in characterization of BC by measurement method is not repeated. Instead, since both measurement types are essentially estimating the same parameter (i.e., BC) albeit via different method orientation, and to make clear that light absorption measurements do not necessarily provide a 'better' indicator of BC than thermal methods, the term BC is used to describe all measurements. In Appendix 1, where this topic is more thoroughly explored, the BC measurements produced by light absorption/optical methods are referred to as apparent BC or "BCa", and those produced by thermal or thermal-optical methods are referred to as apparent EC or "ECa".

Measurement Approaches for BC

The chemical and physical properties of carbonaceous PM vary in terms of both refractivity (the inertness of the carbon at high temperatures) and light absorption. Each carbon measurement technique provides unique information about these properties. All current analysis methods are operationally defined, meaning that there is no universally accepted standard measurement approach. When developing methods and operational criteria to identify BC, some scientists use its optical properties or light-absorbing characteristics (optical or light absorption methods), some use its thermal and chemical stability (thermal-optical methods), while others use its morphology or microstructure or nanostructure (microscopy methods). One major class of methods, thermal or thermal-optical techniques, distinguishes refractory and non-refractory carbon as EC or apparent EC (ECa), and OC or apparent OC (OCa) respectively (see Figure 5-1). The second major class of methods, optical methods, quantifies the light absorbing component of particles as BC or apparent BC (BCa), which can be used to estimate BC concentrations and can also indicate the existence of components that absorb in the near-UV (i.e., brown carbon, BrC). Light absorbing carbon (LAC) is a term used for light-absorbing particles in the atmosphere, which includes BC and BrC.

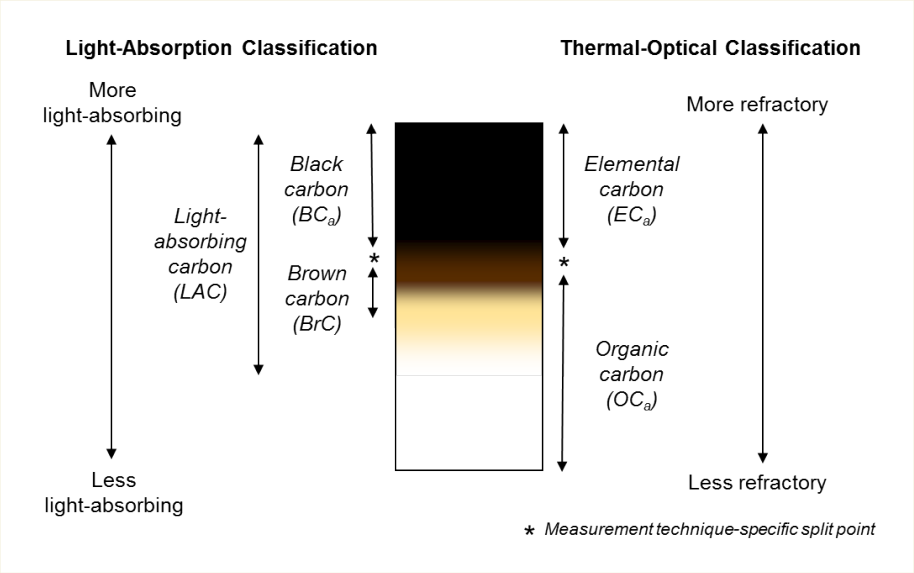

Figure 5-1. Measurement of the Carbonaceous Components of Particles. Black carbon and other types of light-absorbing materials can be characterized by measuring their specific light-absorbing properties, as seen on the left side of the figure (BCa/BrC/LAC). This contrasts with other approaches to characterizing particles based on measurements of the refractory nature of the material (inertness at high temperatures), as seen on the right side of the figure (ECa and OCa). (Source: U.S. EPA)

to measure BC. Filter-based instruments measure the quantity of light transmitted through a filter loaded with particles (Hansen et al., 1982; Lin et al., 1973; Rosen and Novakov, 1983). For filter-based optical instruments, the detected light absorption by particles can be converted to an estimated BC mass concentration. There are two main uncertainties associated with the quantification of filter based BC using optical methods: 1) a filter loading artifact and 2) the selection of an appropriate conversion factor. Several studies have shown that filter-based BC measurement can be affected by the amount and composition of particles loaded onto the filter (Arnott et al., 2005; Collaud Coen et al., 2010; Park et al., 2010; Schmidt et al., 2006; Virkkula et al., 2007; Weingartner et al., 2003). In addition, the selection of the conversion factor to relate light absorption to mass is a significant issue. No single factor is applicable to all methods, wavelengths, particle sizes, particle compositions, shapes and structures. There are a variety of conversion factors that have been published in scientific literature and are commonly applied to estimate BC (Gundel et al., 1984; Liousse et al., 1993; Petzold et al., 1997; Bond and Bergstrom, 2006; Novakov, 1982). Theoretical and empirical studies show that bounds can be placed on absorption efficiencies for different assumptions of BC aerosol origins and composition

(Alfaro et al., 2004; Andreae et al., 2008; Dillner et al., 2001; Cross et al., 2010; Chou et al., 2005; 2009; Favez et al., 2009; Fu and Sun, 2006; Fuller et al., 1999; Horvath, 1993; Jacobson, 2010; Knox et al., 2009; Liousse et al., 1993; McMeeking et al., 2005; Nordmann et al., 2009; Ogren et al., 2001; Ram and Sarin, 2009; Ramana et al., 2010; Rosen and Novakov, 1983; Schuster et al., 2005; Subramanian et al., 2010; Watson et al., 2005; Widmann et al., 2005; Chan et al., 2010). A suggested solution would be to quantify BC in the original light absorption units, which is a strength of the optical techniques. It is recommended that light absorption be reported in the original units of absorption along with any mass absorption coefficients or conversion factors used to convert absorption to BC mass concentration.

While the terms "BC" and "EC" are frequently associated with measurements from the two general categories of specific commercial instruments in the scientific literature, both of these measurement techniques provide estimates of BC concentrations (Wolff et al., 1982; Andreae and Gelencsér, 2006). Ambient monitoring studies that simultaneously utilized light absorption and thermal-optical methods show that the estimates of BC by the two techniques are on average near 1 and generally within 30% (70% of studies had ratios between 0.7 and 1.3); however there do exist studies reporting very low BC:EC ratios (~0.5) and very high BC:EC ratios (~2). Ambient inter-comparison studies have found that estimates of BC from thermal measurement methods are usually reliable predictors of ambient BC estimated via light absorption techniques and vice versa. The comparison of EC by thermal-optical methods and BC by light absorption is sensitive to the source of EC/BC and varies by location. While the estimates from the two techniques are highly correlated and display similar concentration values, they can vary by up to a factor of two among the limited number of studies available.[2] Further discussion of these comparisons can be found in Appendix 1.

5.3 Ambient Concentrations of BC

Currently, few countries have robust networks for ambient measurement of $PM_{2.5}$. Most available global ambient BC data are produced in the United States, Canada, Europe, and China, and the vast majority of these data are based on the more widely available thermal measurement techniques (see section 5.2). In the United States and Europe, limited light absorption measurements are available to supplement these thermal measurements. There is also a modest network of BC monitoring sites across the globe in remote areas to provide information about background levels.

5.3.1 Major Ambient Monitoring Networks

Figure 5-2 provides a map showing the extent of known BC monitoring networks around the globe. The existing networks in the United States, Canada, Europe (EUSAAR, EMEP), and Asia (CAWNET), as well as those with global coverage (GAW, ESRL/GMD) and ad hoc collections of special study data are shown.[3] The map separately shows locations using light absorption, thermal, or both measurement techniques. Most locations shown are in North America and these monitors mostly utilize thermal measurement techniques.

Ambient BC data in the United States are mostly available from $PM_{2.5}$ urban and rural speciation monitoring networks which use thermal measurements. The Interagency Monitoring of Protected Visual Environments (IMPROVE) network started collecting data in 1987, and the urban Chemical Speciation Network (CSN) started in 2001.[4] Urban BC is measured through the CSN network of approximately 200 monitors located in major urban areas.[5] In rural environments such as national parks and wilderness areas, the United States relies on the IMPROVE network to characterize air quality. This network consists of approximately 160 monitors. Like the CSN, the IMPROVE network utilizes thermal measurement technologies.[6] Other U.S. data include supplementary measurements from approximately 45 semi-continuous light absorption monitors (operational in 2007); 5 semi-continuous carbon measurements; and smaller networks of thermal-optical and light absorption monitors (SEARCH, Super-sites). See Appendix 1 for more details. Thermal-optical methods for measuring OC and EC are currently standardized and consistent among the IMPROVE (*http://vista.cira.colostate.edu/improve*),

[2] Comparable studies of the relationship between measured estimates of BC from light absorption and thermal techniques have not been conducted for direct measurements of source emissions.

[3] These BC measurements are publicly available or have been included in peer-reviewed publications.

[4] The VIEWS web site (*http://vista.cira.colostate.edu/views/*) provides information on the start and end dates for each site.

[5] Measurements are based on integrated 24-hr samples, mostly collected every three days, and were mostly analyzed for EC between 2001-2007 using an EPA NIOSH-type TOT protocol. EPA started to transition CSN measurements to the IMPROVE_A TOR protocol for EC in May 2007.

[6] Measured every three days. The IMPROVE program slightly modified the protocol in 2005, which resulted in higher quality data and slightly higher EC as a fraction of total measured carbon. The IMPROVE network data for 2005-2007 are produced using the newer IMPROVE_A TOR protocol.

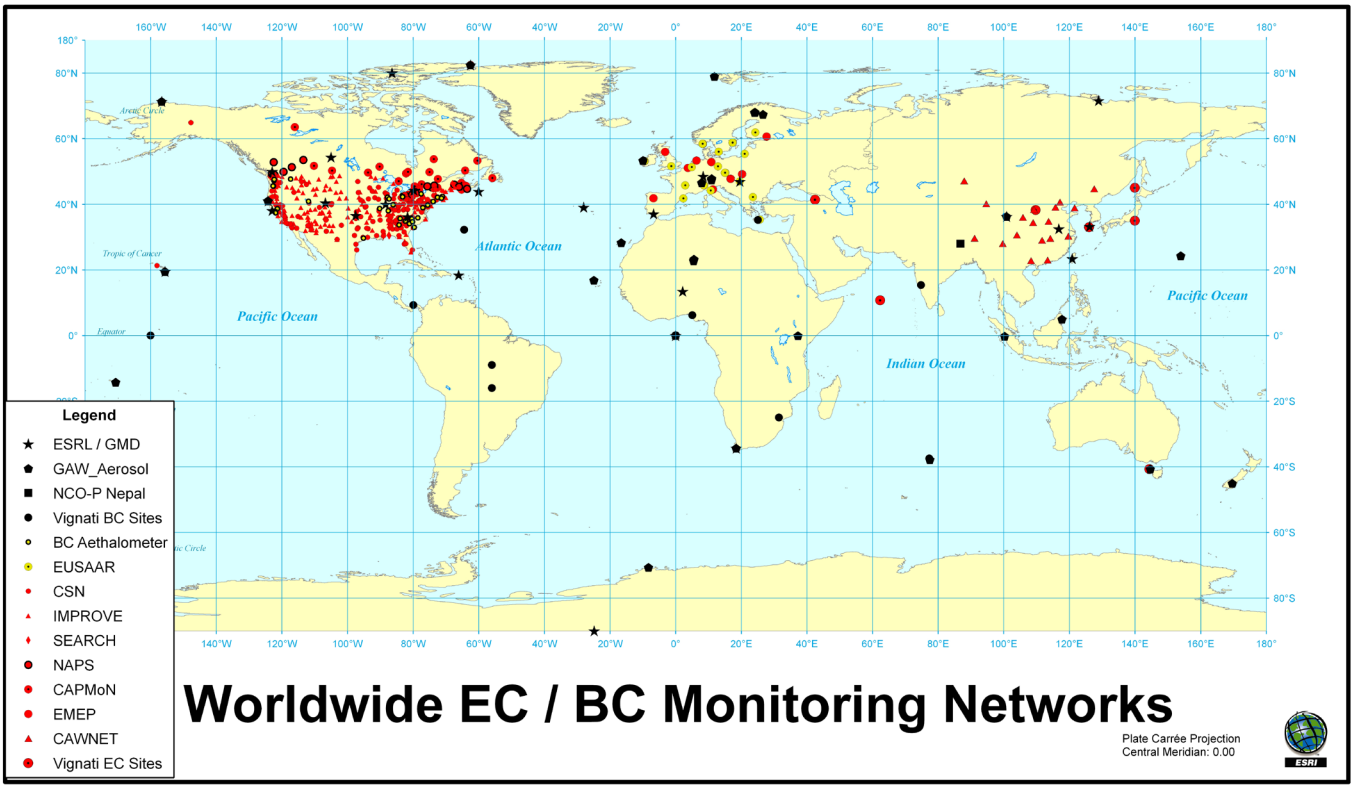

Figure 5-2. Ambient BC Measurement Locations Worldwide. Light absorption measurement locations are colored black. Thermal measurement locations are colored in red. A small subset of locations with both measurements is colored yellow. (Source: U.S. EPA)

CSN (*http://www.epa.gov/ttn/amtic/speciepg.html*), and SEARCH (*http://www.atmospheric-research.com*) networks.

5.3.2 Global Ambient Concentrations

Table 5-2 summarizes data from a number of studies and monitoring networks that help illustrate the range of BC concentrations across the globe. The table also indicates the BC measurement methods (thermal (T) and light absorption (LA)) for each study/monitoring network. While BC measurements for urban and rural areas are similar in North America and Europe, the reported concentrations for China are much higher. Both urban and rural BC concentrations in China are approximately 10 times higher than urban and rural concentrations in the United States, respectively.[7]

The United Kingdom shows higher BC concentrations at the upper range than the United States likely due to the influence of local sources on the individual monitoring sites. In general, roadside or near-source monitors yield higher values, as demonstrated by the curbside monitors in London which report considerably more BC than the urban-wide locations (Butterfield et al., 2010). The "Black Smoke" data for the UK that provide the basis for the five-decade trend discussed in section 4.6.2 are three to four times higher than co-located measurements of BC (Quincey, 2007).

The global background sites that are part of the National Oceanic and Atmospheric Administration (NOAA) network reveal BC concentrations that are one to two orders of magnitude lower than those typically observed in either urban or rural continental locations. The presence of BC in these remote locations without any nearby sources is indicative of long range transport and is used to evaluate intercontinental transport processes in global models.

5.3.3 Comparison of Urban and Rural Concentrations Globally

Available data suggest that BC concentrations vary substantially between urban and rural areas. Specifically, urban areas tend to have higher

[7] As discussed in Chapter 4, the ratio between China and U.S. measured BC concentration is two to three times higher than the ratio of their estimated national BC emissions.

Table 5-2. Summary of Selected Global BC Ambient Concentrations for Urban and Rural/Remote Areas.

Range of Annual Average Concentrations (μg/m³)					
Region	**Networks**	**Year**	**Method Type**	**Urban (# Sites)**	**Rural/Remote (# Sites)**
United States	CSN[a]/ IMPROVE[b] SLAMS[c]	2005–2007 2007	T LA	0.3 to 2.5 (~200 sites) 0.3 to 3.0 (~ 45 sites)	0.1 – 0.6 (~150 sites)
Canada	NAPS[d]	2003–2009	T	0.9 – 1.8 (12 sites)	0.4 – 0.8 (4 sites)
Europe	EMEP[e]	2002–2003	T	1.4 – 1.8 (2 sites)	0.2 – 1.8 (12 sites)
Europe	EUSAAR[f]	2006	T LA	1.5 (2 sites) 2.7 (1 site)	0.1 – 0.7 (4 sites) 0.2 – 0.5 (4 sites)
United Kingdom	BC Network[g]	2009	LA	1.0 – 2.9 (19 sites)	
China	CAWNET[h]	2006	T	9.3 – 14.2 (5 sites)	0.3 – 5.3 (13 sites)
Nepal	NCO-P[i]	2006–2008	LA		0.16 (1 site)
Global Background	NOAA GMD Sites[j] Mauna Loa Point Barrow South Pole	 1990–2006 1988–2007 1987–1990	 LA LA LA		 0.01 – 0.02 0.02 – 0.07 0.002 – 0.004
Other Arctic Sites	Alert (Canada) Zeppelinfjell[f] (Svalbard, Norway)	1989–2008 2002–2009	LA LA		0.04 – 0.1 0.02 – 0.06
United Kingdom	Black Smoke (BS)[k]	2006	LA	5.0 – 16.0 (12 sites)	

[a] CSN – Primarily urban network sites.

[b] IMPROVE – Rural network sites.

[c] BC data at State and Local Air Monitoring Stations from AQS, mostly with Magee Aethalometers.

[d] Personal communication with Tom Dann (Environment Canada).

[e] Monitoring was for the period 07/02 – 06/03 from Yttri et al. (2007).

[f] Data taken from *http://ebas.nilu.no/* or EUSAAR, the sites assigned to be urban are Ispra, IT (BC) and Melpitz, DE. Although not part of EUSAAR, the urban sites also include Ring A10, NL (EC). The northern EUSAAR remote location of Zeppelinfjell, NO, site is included with other Arctic sites listed separately.

[g] Urban network sites from Butterfield (2010); Curbside site at London Marylebone Road reported 10μg/m3.

[h] Data and urban/regional/remote classification was for the period 2006 from Zhang et al. (2008).

[i] Monitoring was for the period 03/06 – 02/08 from Marinoni et al. (2010).

[j] NOAA Global Monitoring Division Sites – For this table, we modified reported numbers in absorption units using a nominal mass extinction coefficient of 10m2g-1. One year from each site was eliminated as non-representative.

[k] Data taken from *http://www.airquality.co.uk/reports/cat05/1009031405_2009_BC_Annual_Report_Final.pdf*; curbside site at London Marylebone Road reported an average of ~40μg/m3 for each year.

concentrations. The global BC data (for 2005-2007 average or calendar year 2006) displayed in Figure 5-3 contrast the annual average rural and urban concentrations for North America, China, and Europe.[8, 9] The ambient rural concentrations provide an indicator of regional background concentrations resulting from regional emissions and transported aerosols. Levels in urban areas reflect the higher average concentrations resulting from the combination of local emissions and regional emissions. The portion of urban concentrations due to local emissions can also be described as the "urban increment" or "urban excess".[10]

[8] The data in Figure 5-3 are aggregated and displayed on the 1.9 x 1.9 degree resolution which is widely used by global climate models. This coarse grid does not allow us to see sharp gradients which tend to exist within urban areas. Also, note that these grid-based displays use a logarithmic scale to show the order of magnitude range of concentrations for BC across the globe.

[9] The map in Figure 5-3 shows the 40th parallel, the importance of which is discussed further in Chapter 4.

[10] Because of strong regional homogeneity among background measurements, urban grid squares without measurements were estimated from nearby cells to permit an estimate of urban excess. These estimated values may be higher than surrounding regional measurements. Spatial interpolation here is based on inverse distance weighting of the nearest neighbors (Abt Associates, 2005).

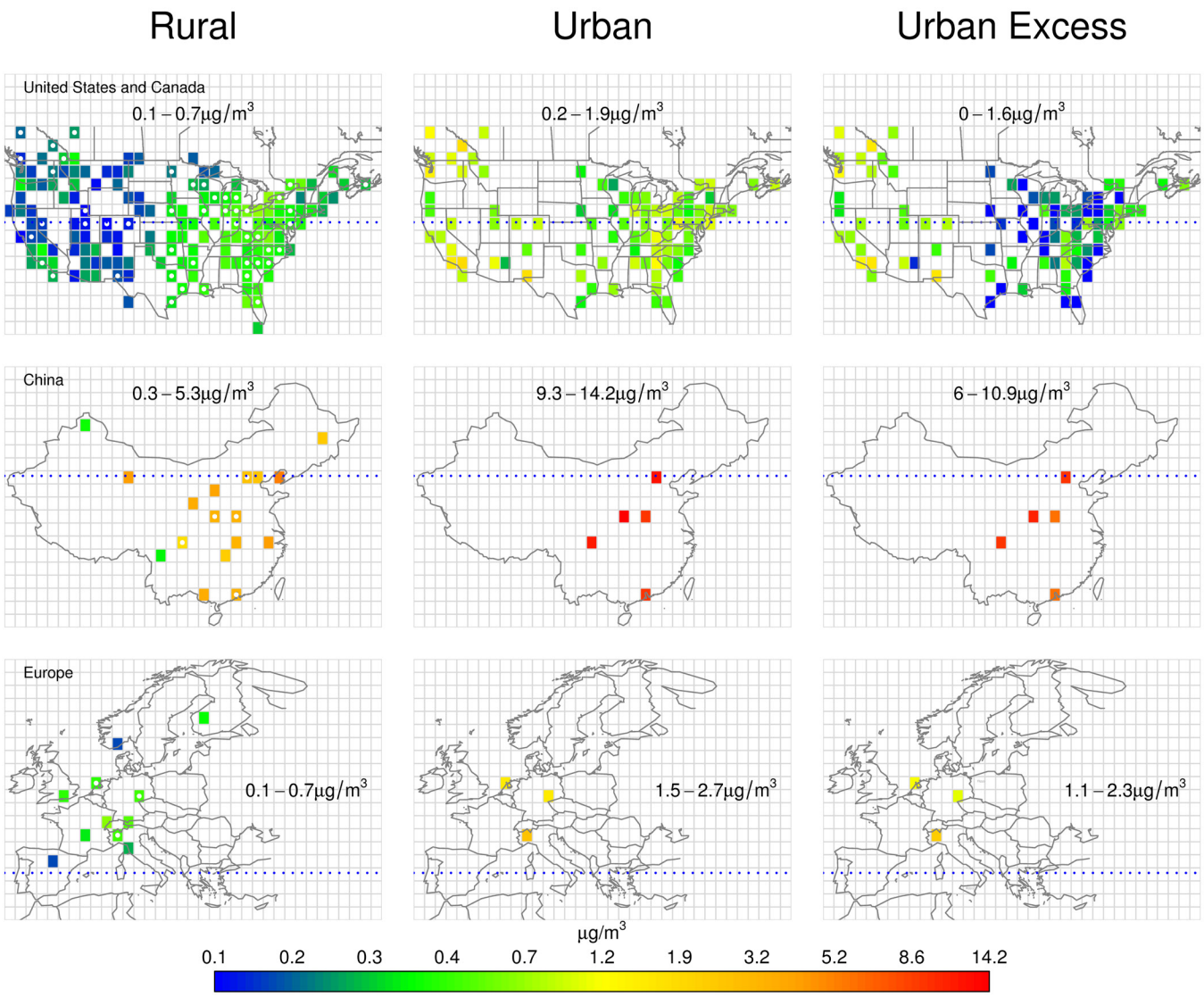

Figure 5-3. Spatial Distribution of Global BC Data. Rural, urban, and urban excess concentrations for 2005-2007. Grid squares with a white dot represent estimated rural concentrations from spatial interpolation of the nearest neighbors with measurement data. The 40th parallel is shown as a dotted line. (Source: U.S. EPA)

As demonstrated in Figure 5-3, urban BC measurements in North America are generally much higher than the nearby regional background levels. This suggests that there can be a substantial increment of local emissions in urban areas. For the period 2005 to 2007, the urban increment ranged from zero to 2.2 µg/m^3 (i.e., up to 92% of the total urban BC concentrations). In general, average urban concentrations are relatively consistent across North America, though the larger populated regions of the eastern United States, eastern Canada, and California contain most of the highest concentrations. However, the western United States and western Canada have lower regional background concentrations and therefore relatively larger urban increments, while higher rural concentrations in eastern North America result in smaller urban increments (more similar regional and urban average values). The higher regional background levels across eastern North America suggest higher and more consistent levels of BC emissions from sources across the region, and/or greater transport from clustered cities to surrounding rural areas.

Figure 5-3 also shows that Europe's measurement data are quite similar to those for North America. However, both China's regional and urban BC concentrations are much higher than those seen in

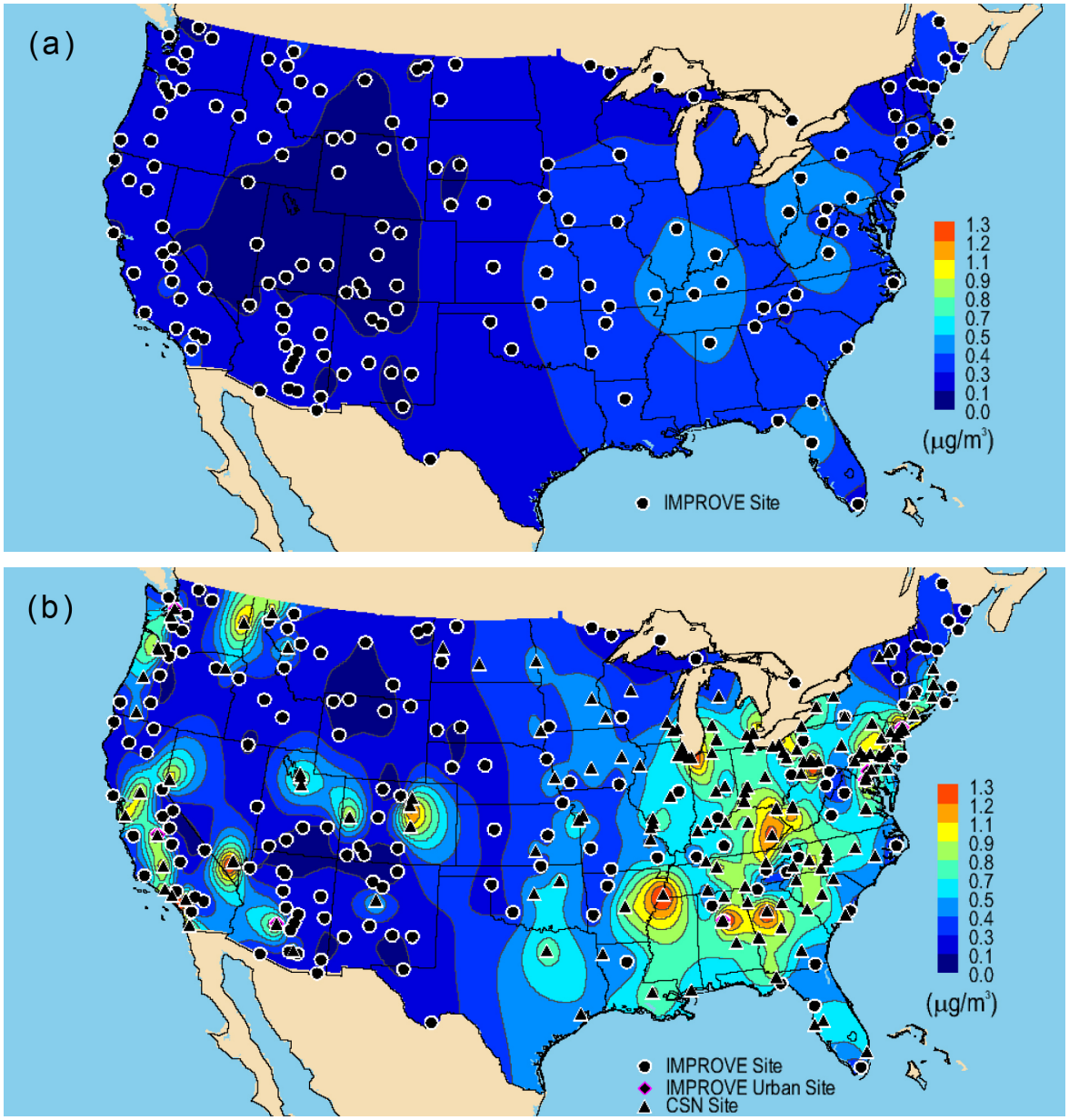

Figure 5-4. Annual Mean BC Concentrations (µg m^{-3}) for 2005–2008 in the United States. Panel (a) shows rural EC concentrations provided by IMPROVE network. Panel (b) shows the combined rural IMPROVE and urban CSN network EC data. IMPROVE site locations are shown as black circles, CSN sites are shown as black triangles, and urban IMPROVE sites are shown as magenta diamonds. (Adapted from Figures 7.5.1 and 7.5.2 of IMPROVE report V (2011) *http://vista.cira.colostate.edu/improve/*)

North America and Europe and its urban increments are approximately four times larger. This can be attributed in part to larger urban and regional emissions sources in China compared to North America and Europe.

To provide additional spatial detail to U.S. BC concentrations, Figure 5-4 shows the spatial distribution of background and combined urban plus background concentrations derived from EC measurements in the IMPROVE and CSN monitoring programs. While the background concentrations are relatively homogeneous over large sub-regions of the United States, Figure 5-4(a) indicates these background concentrations are generally higher in the Industrial Midwest. As shown in Figure 5-4(b), urban areas have much higher concentrations. High ratios of urban to rural BC concentrations

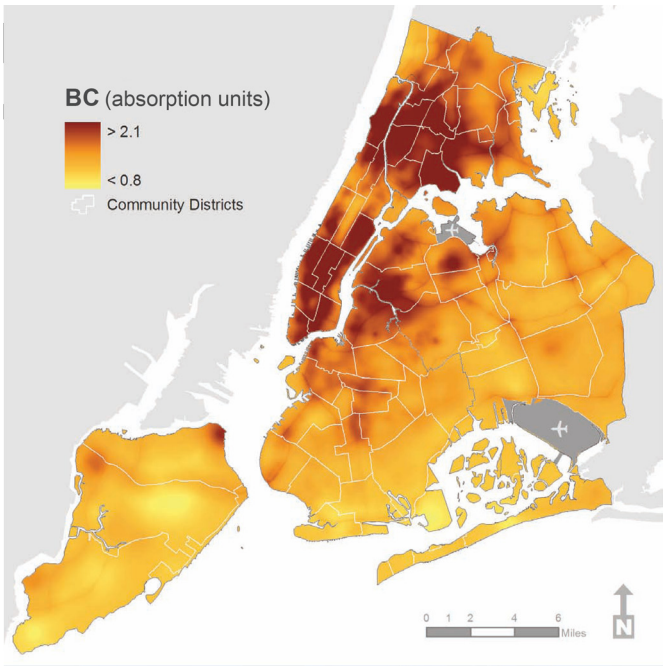

Figure 5-5. Urban BC Gradients for New York City. (Source: The New York City Community Air Survey, Results from Winter Monitoring 2008-2009, *http://www.nyc.gov/*)

demonstrate the localized impact of BC on surrounding rural regions and suggest urban BC emissions sources were significantly larger than rural sources. The mean urban to rural ratio was 3.3 ± 1.9 and was much larger than the mean ratio for sulfate, nitrate, or OM components of $PM_{2.5}$ (Hand et al., 2011).

In addition to the general contrast between measured urban and nearby rural BC concentrations, there can be substantial spatial variation in BC concentrations within a given city. Because global representations of BC concentrations are typically based on limited monitoring locations and are generally presented as average concentrations (often across monitors hundreds of miles apart), it is important to realize that ambient concentrations of BC in any urban area can vary widely from location to location within the city. BC concentrations can vary spatially within an urban area because the magnitude of monitored BC concentrations is dependent on the proximity of the monitor to roadways and other nearby sources. Therefore, concentrations measured may not be representative of other locations. Figure 5-5 illustrates the estimated spatial variability of BC in New York City.[11] This special study used 150 monitoring sites to reveal large gradients in apparent BC concentrations. Actual gradients may even be larger. Furthermore, the illustrative within-urban variability for NYC may also be representative of other urban areas with high population and emissions density. While most of the identified high concentration zones can be attributed to mobile source emissions density, this study also revealed significant BC emissions sources associated with residential oil combustion.

5.3.4 BC as a Percentage of Measured Ambient $PM_{2.5}$ Concentrations in the United States

Because total $PM_{2.5}$ mass is the basis for regulation of fine particles in the United States and also serves as the basis for BC emissions estimates, it is informative to estimate the contribution to total $PM_{2.5}$ mass from BC. However, given the limited BC data available on a global scale, this evaluation is based solely on data for urban areas in the United States that are regionally representative of large U.S. cities. Compared to U.S. rural locations, urban locations contain a higher percentage of BC and OC. While urban nitrate concentrations are also higher than surrounding rural areas, carbonaceous aerosols are responsible for most of the urban $PM_{2.5}$ increment. Other components, such as dust, are similar in both urban and rural environments (U.S. EPA, 2004b). Figure 5-6 shows the BC fraction of $PM_{2.5}$ mass for 15 selected U.S. urban areas. The values represent average concentrations among monitoring locations in the area. The average BC concentrations range from 0.6 µg/m^3 in St. Louis to 1.2 µg/m^3 in Atlanta. The percentage of $PM_{2.5}$ that is BC ranges from 4% in St. Louis to 11% in Seattle.[12] A more complete characterization of urban and rural $PM_{2.5}$ speciation components on an annual and seasonal basis can be found elsewhere (Hand et al., 2011; U.S. EPA, 2009b).

[11] Based on 150 filter-based portable samplers and optical absorption measurements with the smoke stain reflectometer.

[12] Approximately 20-80% of the estimated ambient organic matter (OM) is directly emitted (Carlton et al., 2009). The other portion, termed secondary organic aerosol (SOA), is formed through chemical reactions of precursor emissions after being released from the sources (Saylor et al., 2006; Carlton et al., 2009; Chu, 2005). OM is typically 1.4 to 1.8 times higher than measured OC levels in urban areas, with an even larger multiplier of OC levels measured in rural areas (Bae et al., 2006; Turpin and Lim, 2001). The OM-to-OC ratio tends to be higher with an aged aerosol (resulting from transported, atmospheric-processed, and aged particles), SOA, or directly emitted OM from biomass combustion. Although we are not able to quantify the amount of OM that may be BrC, it is worth noting that average OM for the 15 selected cites represents 26% to 55% of $PM_{2.5}$ and the OM-to-BC ratio ranges from 4 to 9.

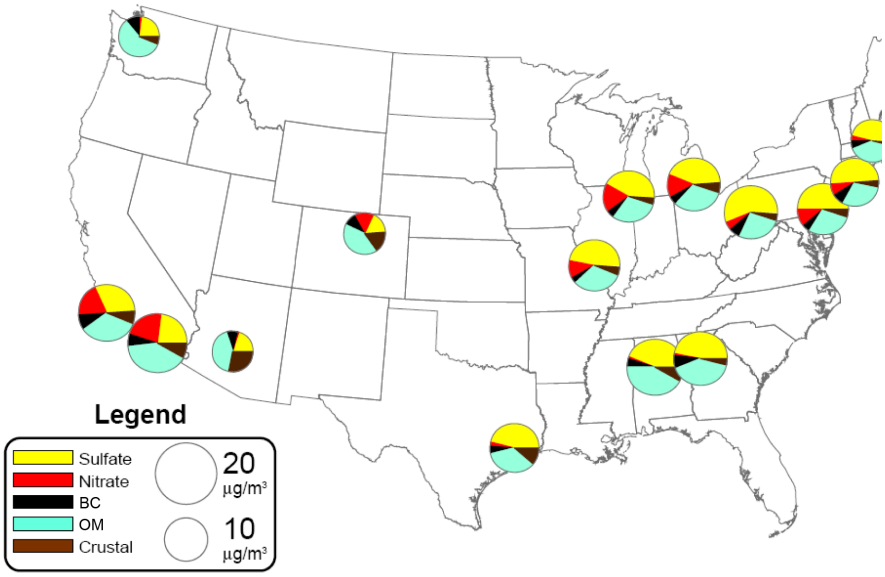

Figure 5-6. Composition of $PM_{2.5}$ for 15 Selected Urban Areas in the United States. Annual average $PM_{2.5}$ concentrations (µg/m^3) are presented where the circle size represents the magnitude of $PM_{2.5}$ mass. The BC and Organic Mass (OM) fractions are illustrated. OM represents OC together with its associated non-carbonaceous mass (e.g., hydrogen, oxygen and nitrogen), estimated by a material balance approach. Sulfates and Nitrates have been adjusted to represent their mass in measured $PM_{2.5}$. (Source: U.S. EPA, 2009b)

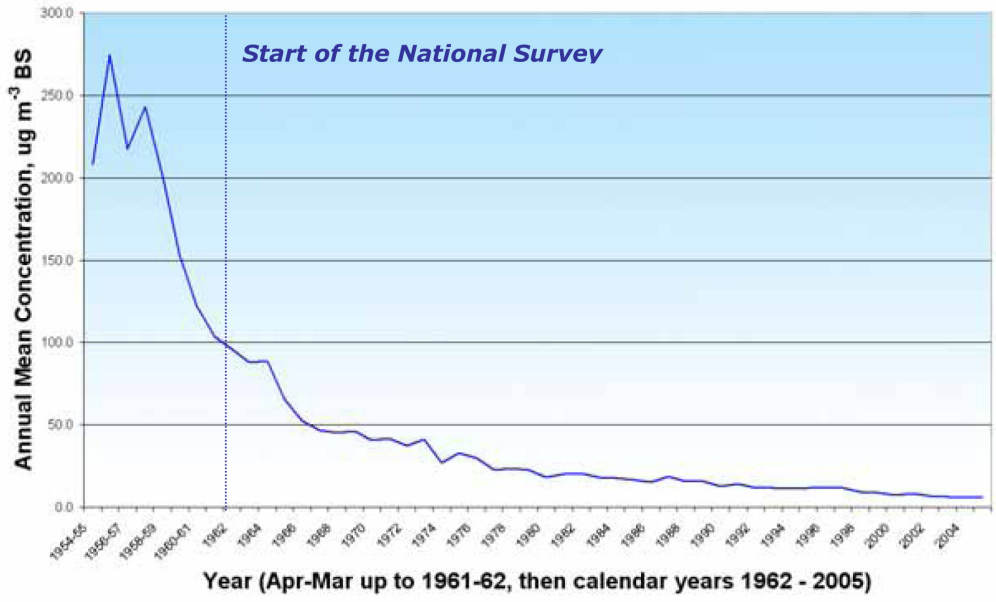

Figure 5-7a. Trends in Black Smoke Measurements (µg/m^3) in the United Kingdom, 1954-2005. The BS measurements are highly correlated with optical BC, although BS is 3 to 4 times higher than BC under current U.K. aerosol conditions. In 1961, the UK established a national air pollution monitoring network, called the National Survey, monitoring black smoke and sulphur dioxide at around 1,200 sites in the UK. (Bower et al., 2009)

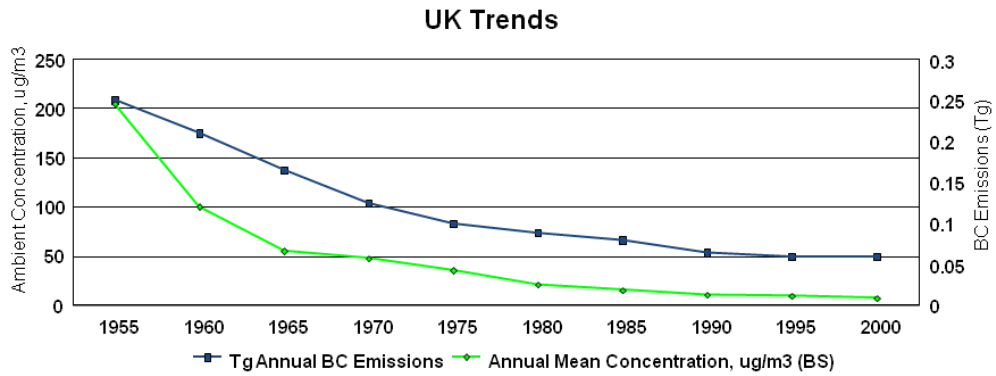

Figure 5-7b. Comparison of Ambient Black Smoke Measurements (µg/m^3, annual average) with Estimated BC emissions (Tg) in the United Kingdom, 1955-2000. (Source: U.S. EPA)

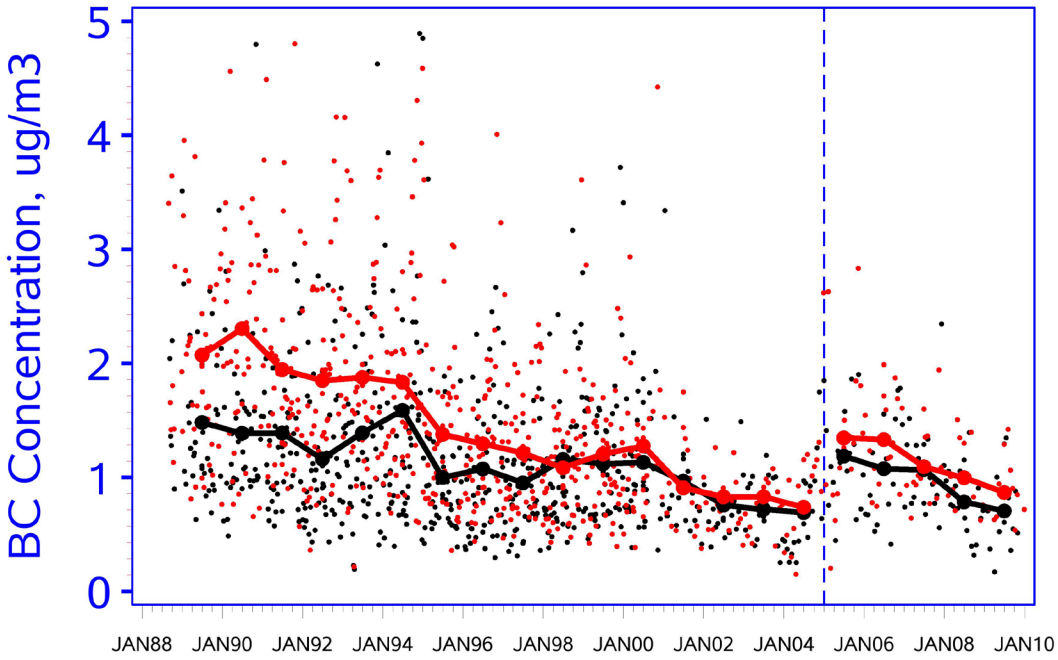

Figure 5-8. Ambient BC Trends in Washington, D.C. The red data points and line represent daily and annual average concentrations from Wednesdays (as a proxy for weekdays) and the black data points and line represent daily and annual average concentrations from Saturdays (as a proxy for weekends). The large dots represent the annual average concentration which is plotted at mid-year. This monitoring site changed its sampling protocol from twice per week (Wednesday and Saturday) to once every 3 days in August 2000. The apparent increase in BC concentration after January 2005 coincides with a carbon analyzer upgrade resulting in total carbon measurements with a higher proportion of BC. (Source: U.S. EPA, produced using data from VIEWS *http://vista.cira.colostate.edu/views*)

Note: The potential increase in reported EC measurements is described by White (2007), *http://vista.cira.colostate.edu/improve/Data/QA_QC/Advisory/da0016/da0016_TOR2005.pdf*.

5.4 Trends in Ambient BC Concentrations

5.4.1 Trends in Ambient BC Concentrations in the United States and the United Kingdom

Measurement data necessary for assessing long-term ambient trends in BC are limited even for the areas with currently robust monitoring programs such as the United States.[13] However, although limited, some information on changes in ambient concentrations over longer time periods is available and these data are useful in evaluating and corroborating emissions trends. Since most BC is directly emitted rather than the formed chemically from precursors in the atmosphere, ambient BC concentrations respond directly to emissions changes. Figure 5-7a shows the dramatic reduction in measured "Black Smoke" (BS) in the UK since the 1950s. This dramatic decline is attributable to a number of factors, including the introduction of cleaner fuels and technologies, and successful smoke control legislation (Bower et al., 2009). Figure 5-7b overlays these BS measurements and estimated BC emissions for the UK for the same time period, revealing large estimated emissions reductions corresponding to 80% of the reduction in black smoke.

For more recent time periods, there is a great deal more data available to assess ambient trends in the United States than there is for longer-term historical trends. A variety of measurements from the IMPROVE and CSN networks, as well as other monitoring locations, provide important data for assessing recent changes in ambient BC

[13] Assessment of longer term trends in BC is possible by analyzing ice core and lake sediment data. These data reflect historical archives from which BC concentrations can be estimated and used to supplement more recently available direct ambient air quality measurements. A discussion of these data and the corresponding results is the focus of section 5.6 of this chapter.

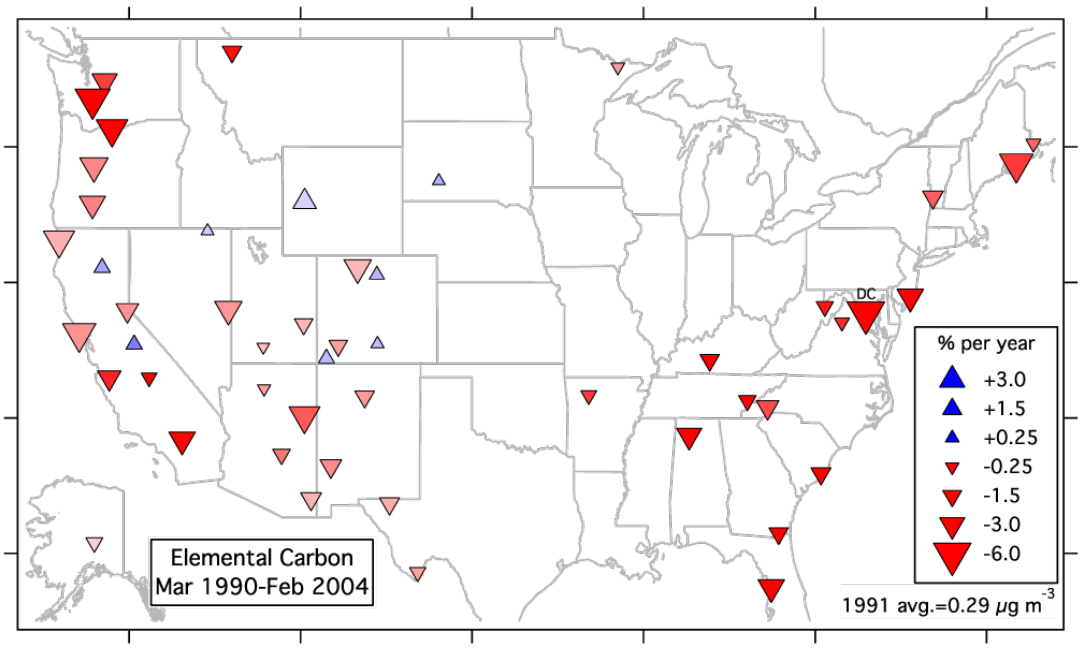

Figure 5-9. Trends in BC at All IMPROVE Network Stations with Sufficient Data between 1 March 1990 and 29 February 2004. Marker size indicates the magnitude of the trend. Triangle direction and blue or red color corresponds to the sign of the trend. Color saturation is proportional to the average concentration in 1991 with full saturation at twice the national median. The only urban site in Washington, D.C. is marked. Averages in the bottom right corner exclude Washington, D.C. (Adapted from Murphy et al., 2011)

concentrations domestically. Figure 5-8 shows the 1988-2009 (22-year trend) for BC in Washington, D.C. as measured by the IMPROVE program. IMPROVE's urban Washington, D.C. monitoring site has one of the longest BC monitoring records in the United States. These data are presented as separate time series due to a change in the frequency of sampling and with a separation at the end of 2004 due of an upgrade to newer analytical equipment. The trends show a substantial two decade decline in ambient BC concentrations. The percent change in Washington, D.C.'s BC on Wednesdays and Saturdays was 62% and 49% respectively, based on a comparison of average levels in 1989-1991 compared to 2002-2004, and 54% and 40% comparing 1989-1991 with 2007-2009. The higher BC concentrations and more substantial BC reductions during the week as compared to the weekend may correspond to the influence of the reduction in diesel emissions.

Nationwide reductions in average BC concentrations have also been observed in rural areas during this same time period (Figure 5-9). BC concentrations in the rural United States decreased by over 25% between 1990 and 2004. Although not shown in this figure, percentage decreases were much larger in winter, suggesting that emissions controls have been effective in reducing concentrations across the entire United States (Murphy et al., 2011). The large 22-year urban BC decline illustrated for Washington, D.C. may in fact be larger than the overall estimated nationwide reductions in BC and direct $PM_{2.5}$ emissions in the United States described in Chapter 4, and is the result of area-specific emissions dominated by certain emissions sectors.[14]

Figure 5-10 juxtaposes estimated annual average BC concentrations in the San Francisco Bay with annual consumption of diesel fuel in California (Kirchstetter et al., 2008).[15] Kirchstetter notes that the contrast in the trends in BC concentration and diesel fuel use is striking, especially beginning in the early 1990s when BC concentrations began markedly decreasing despite sharply rising diesel fuel consumption. This contrast suggests that control technologies to reduce BC emissions have been successful (see

[14] As stated in Chapter 4, national BC emissions decreased by 79%, 30%, and 25% for on-road gasoline, on-road diesel, and nonroad diesel sources, respectively, from 1990 to 2005. Also, Chapter 8 (Table 8-1) shows that 45% of the on-road BC reductions are due to gasoline vehicles. Thus a combination of on-road gasoline and diesel are each potential contributors to the lower BC in our nation's capital and other urban areas.

[15] BC was estimated using Coefficient of Haze (COH) measurements, which are shown to be highly correlated with optical BC. See Appendix 1 for further details regarding COHs.

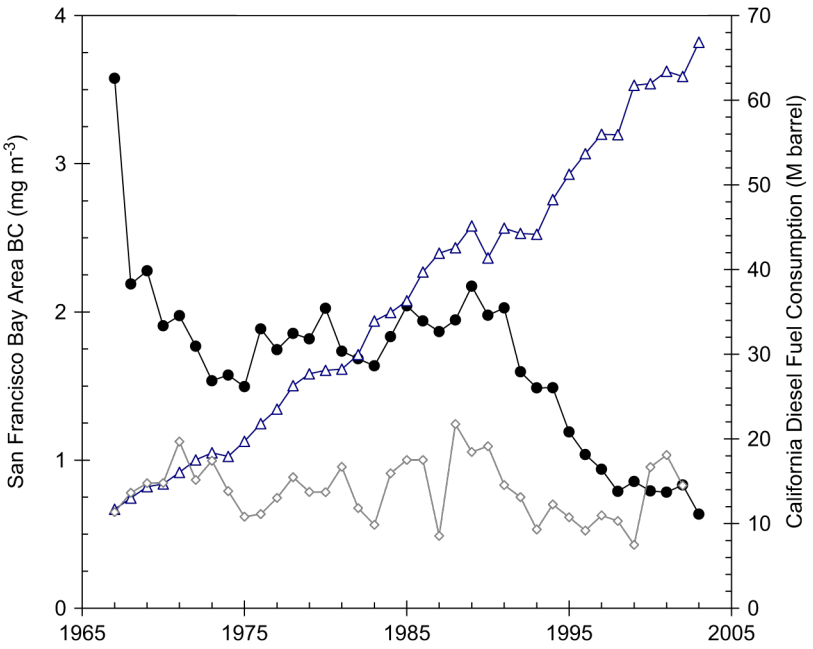

Figure 5-10. Estimated Annual Average Ambient BC Concentrations in the San Francisco Bay Area vs. Diesel Fuel Consumption. BC is shown as black dots. California on-road (blue) and nonroad (gray) diesel fuel consumption are shown as triangles and diamonds. (Kirchstetter et al., 2008)

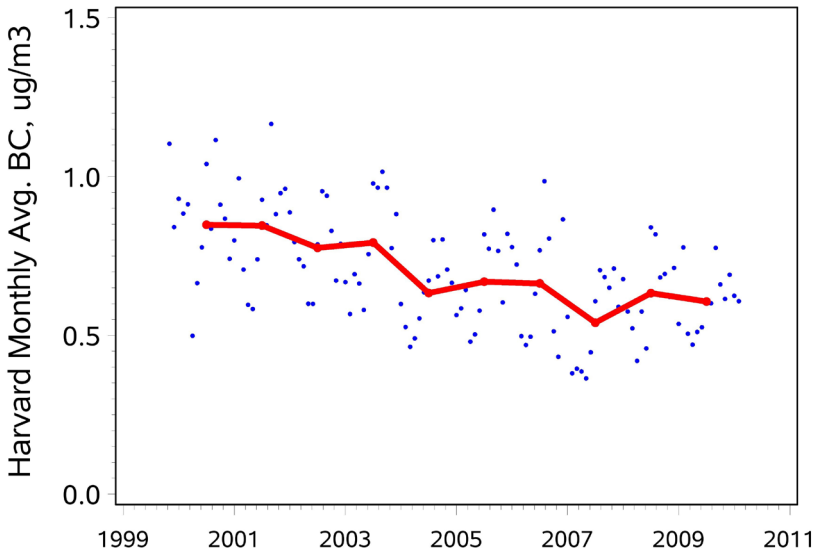

Figure 5-11. Ambient BC Trends in Boston (Harvard School of Public Health location). The blue squares are monthly averages and red line is the annual average of BC concentrations as directly reported by an Aethalometer. (These data were not adjusted using correction algorithms described in Appendix 1.) (Source: U.S. EPA, data courtesy of Harvard School of Public Health)

Chapter 8). Similarly, Figure 5-11 shows a data set from Boston, MA which displays a decline in BC concentrations during the period 2000-2009. These data are presented as monthly average concentrations to help reveal the underlying trend, but much higher temporal variability exists in the 5-minute or even hourly concentrations which respond to patterns in nearby mobile emissions and can even identify when a diesel truck passes by. The decline of BC concentration at this site has been attributed to diesel retrofits in Boston, but is no doubt also reflective of fleet wide changes in emissions especially due to diesel emissions standards (U.S. EPA, 2004c).

Figure 5-12 shows that BC concentrations have declined 32%, on average, for a 15-site subset of EPA's national urban CSN monitoring sites with the longest historical record. The figure shows the range of monthly average BC concentrations represented by CSN EC measurement data. Because EPA transitioned its urban EC monitoring to the IMPROVE protocol, CSN EC measurements have been produced by two different monitoring protocols. As discussed in section 5.2, EC may vary by a factor of two and in fact, that may also be true for these two data records. Therefore, the concentration data for these sites (which were all part of the first group which switched from the older CSN NIOSH-type monitoring protocol) are shown as reported after May 2007 while the earlier data are adjusted to be IMPROVE-like.[16] The details about this adjustment are described in Appendix 1. In general, the CSN sites and trend are representative of neighborhood, urban-wide, and regional-scale emissions influences and may not necessarily reflect local scale emissions changes. Nevertheless, the range of monthly average concentrations among the group of 15 urban locations illustrates

[16] As discussed in Appendix 1, the adjustments are based on parallel measurements at 14 urban IMPROVE and 168 urban CSN locations between 2005 and 2011; the adjustment and trend prior to 2005, therefore, is more uncertain.

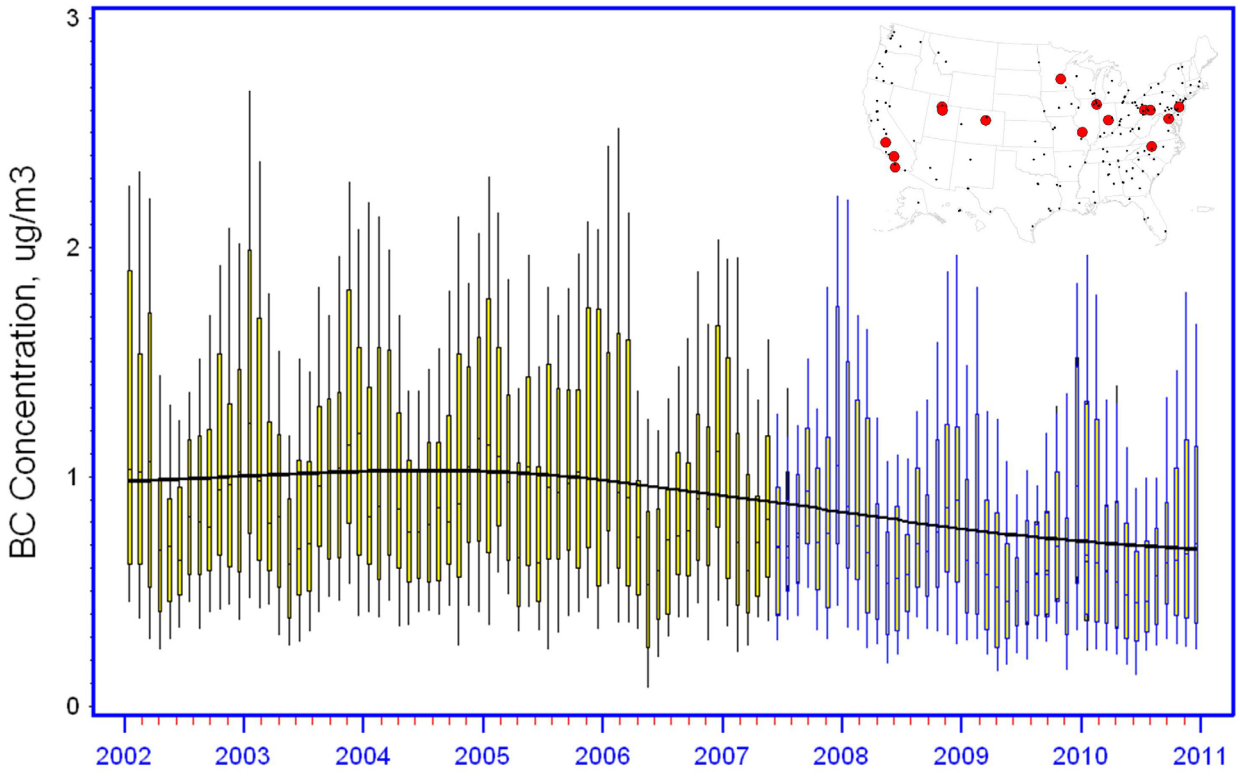

Figure 5-12. Ambient BC Trends (2002-2010), based on monthly distribution of average concentration among 15 CSN monitoring locations in the United States. The map shows the location of the 15 monitoring sites. Starting May 2007, the measured EC were produced with the IMPROVE monitoring protocol. The data prior to May 2007 were produced with the EPA NIOSH-type protocol and adjusted to represent the IMPROVE protocol. For a more detailed explanation of this graphic, see Appendix A, Figures A1-6 and A1-7 and surrounding text. (Source: U.S. EPA)

seasonal variability in BC. However, the higher winter BC concentrations, which may be due to local emissions patterns or climatology, were not evident at all sites and geographic regions.

Based on the evidence provided above from a variety of recent BC indicator measurements (and derived from different data sources), it appears that ambient concentrations of neighborhood/urban and regional scale concentrations of BC in the United States substantially declined from the mid 1980s. The urban and regional BC declines can generally be attributed to emissions reductions associated with engine and fuel improvements (Bahadur et al., 2011; Kirchstetter et al., 2008; Minoura et al., 2006; Murphy et al., 2011) and reductions in residential biomass burning emissions (Burnet et al., 1988; Butler, 1988; Hough, 1988) to attain NAAQS (Bachmann, 2007) for PM and other pollutants.

5.4.2 Trends in Ambient BC Concentrations in the Arctic

Trends in BC concentrations at three Arctic locations (Alert Canada, Barrow Alaska, and Zeppelin Norway) are presented in Figure 5-13 (Hirdman et al., 2010). As stated by the authors, there is a general downward trend in the measured BC concentrations at all stations, with an annual decrease of −2.1±0.4 ng/m^3 per year (for the years 1989-2008) at Alert and −1.4±0.8 ng/m^3 per year (2002-2009) at Zeppelin. The decrease at Barrow is not statistically significant. Based on transport analysis the authors conclude that northern Eurasia (the NE - Northeast, WNE - West Northeast, and ENE - East Northeast clusters) is the dominant emissions source region for BC and decreasing emissions in this region drive the downward trends. However, there are indications that the BC emissions from ENE in wintertime have increased over the last decade, probably reflecting emissions increases in China and other East Asian countries. Emissions associated with the other

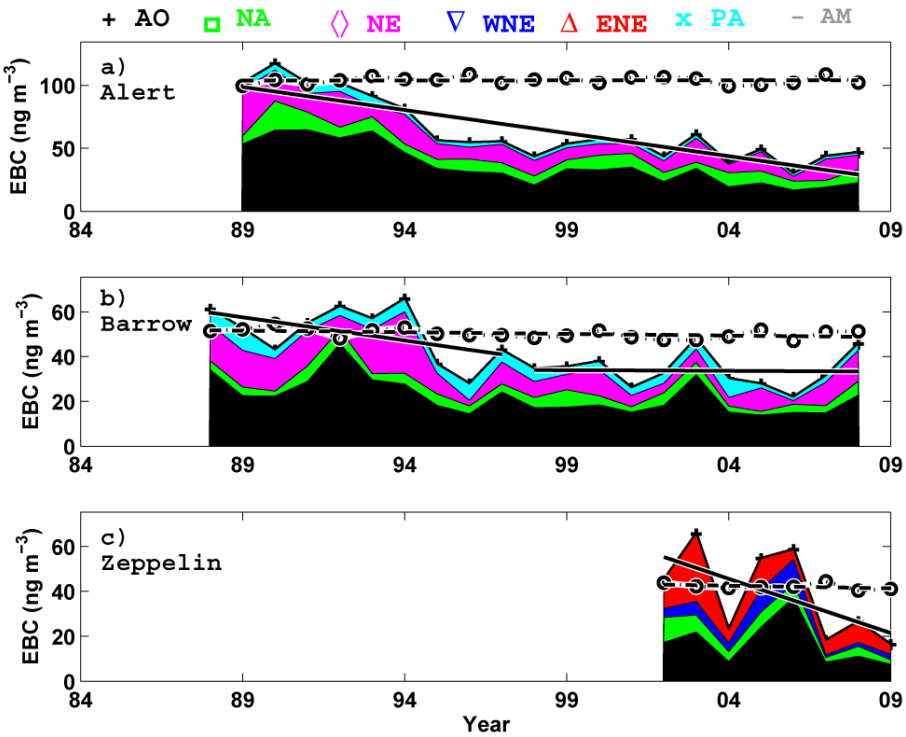

Figure 5-13. The Annual Mean BC Concentrations Measured at Alert (a), Barrow (b), and Zeppelin (c) and Split into Contributions from the Four Transport Clusters. The annual mean concentrations measured at Alert (a), Barrow (b), and Zeppelin (c) are split into contributions from four transport clusters. The solid line shows the linear trend through the measured concentrations. The circles show the annual mean BC concentrations when the cluster-mean concentrations are held constant over time (means over the first three years). This line is influenced only by changes in the frequencies of the four clusters. The dashed line shows the linear trend of these data. (Hirdman et al., 2010)

clusters (Arctic Ocean - AO, North America - NA, Pacific-Asia - PA, and west northeast Eurasia - WNE) have been stable or decreasing over the time periods in this study.

5.5 Remote Sensing Observations

Measurements from satellite and ground-based remote sensing are useful in describing global aerosol and, in particular, BC absorption. Satellites systems designed with aerosol remote sensing capability include MODIS and MISR on Terra and Aqua, as well as GLAS and CALIPSO lidars which describe aerosol layer heights and other satellite instruments such as the Total Ozone Mapping Spectrometer (TOMS) (Winkler et al., 2007). The ground-based remote-sensing Aerosol Robotic Network (AERONET) has provided information on aerosol distribution, seasonal variation and absorption properties since 1963 (Holben et al., 1998; Kahn et al., 2010; 2007; 2009; Kazadzis et al., 2009).

Unlike spatially discrete ambient BC monitors, remote sensing observations are global and thereby offer greater spatial surface coverage of BC levels and provide important estimates of BC where surface ambient measurements are not available. While remote sensing does not necessarily characterize surface concentrations, it provides important information on spatial variability of concentrations in BC and aerosols throughout the total atmospheric column. Combining these new data sources with traditional ground based (ambient) measurements has been used to derive the complete aerosol effect on the environment and climate (Falke et al., 2001; Husar, 2011). Integrated data sets of aerosol based extinction have relied heavily on AERONET sun photometer measurements in remote locations with low concentration and relatively homogeneous aerosol (Kaufman et al., 2001), while downwind of pollution or dust sources they have relied on MODIS characterization of the aerosol spatial distribution over the ocean and dark surfaces (Remer et al., 2002) and on TOMS over bright surfaces (Torres et al., 2002).

AERONET derived estimates of total column aerosol optical depth (AOD) at 4 wavelengths (440, 670, 870 and 1020) can further characterize other aerosol optical properties, including an estimate of Aerosol Absorption Optical Depth (AAOD) throughout the absorption spectrum (Holben et al., 1998; Dubovik and King, 2000). Similarly, aerosol measurements from the Ozone Monitoring Instrument (OMI) of TOMS also provide a measure of AAOD.

Koch compares estimated AAOD for 1996–2006 based on AERONET with OMI satellite retrievals for 2005–2007 (Koch et al., 2009; Torres et al., 2007). Koch notes that the two data sets broadly agree with one another. However, the OMI estimate is larger than the AERONET value for South America (with UV sensitive biomass combustion) and

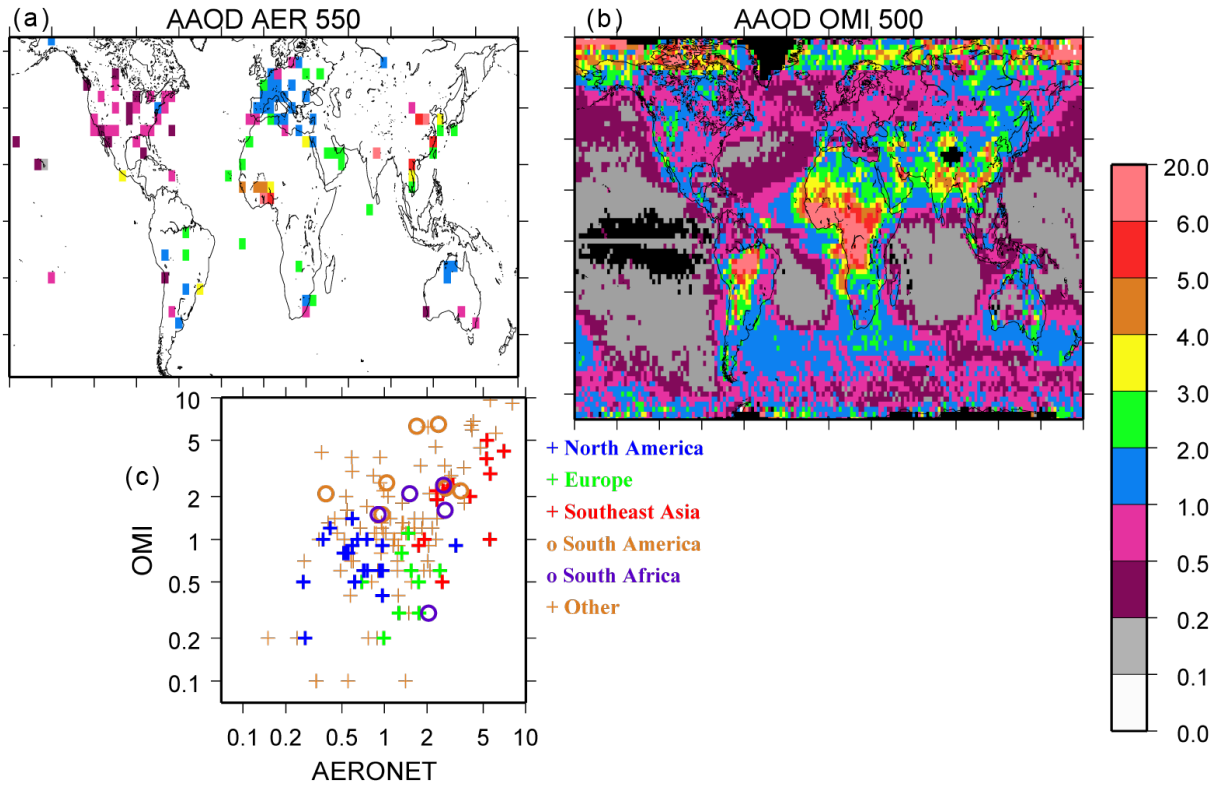

Figure 5-14. Aerosol Absorption Optical Depth (AAOD) from AERONET (1996-2006) and OMI (2005-2007). (a) Aerosol absorption optical depth, AAOD, (x100) from AERONET (at 550 nm), (b) OMI (at 500 nm) and (c) scatter plot comparing OMI and AERONET at AERONET sites. (Koch et al., 2009)

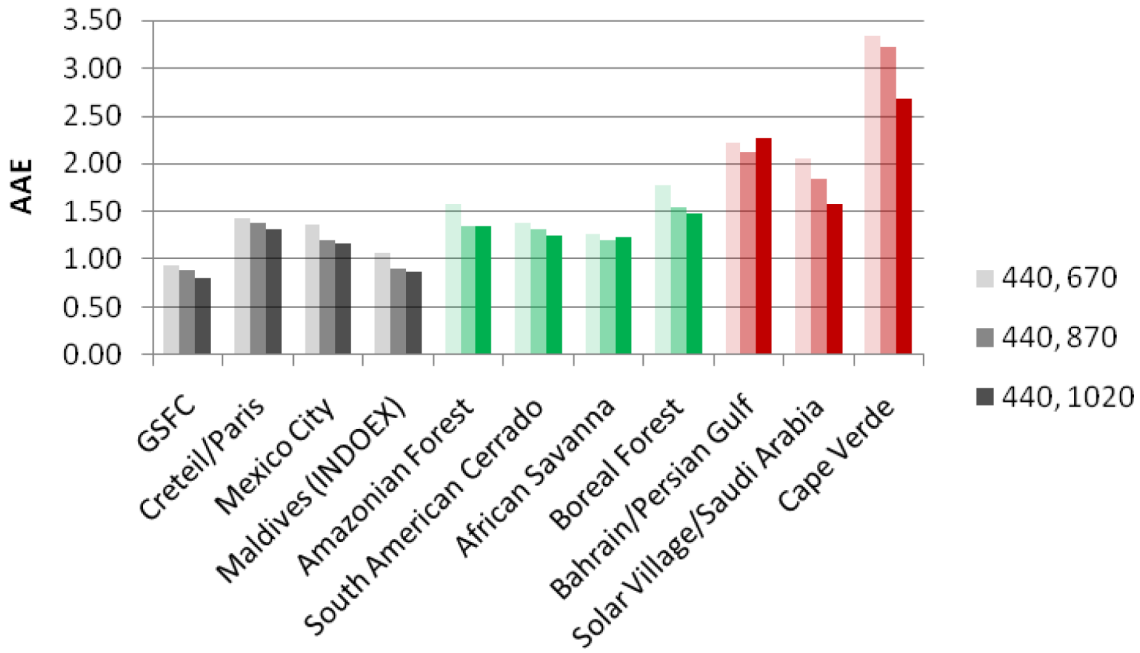

Figure 5-15. Absorption Angstrom Exponent (AAE) Values for AAOD Spectra Derived from AERONET Data. Black: Urban/Industrial or Mixed; Green: Biomass Burning; Red: Desert Dust. Shading for each location indicates wavelength pair (in nm) for AAE calculation. GSFC=Goddard Space Flight Center, Greenbelt, MD. (Russell et al., 2010)

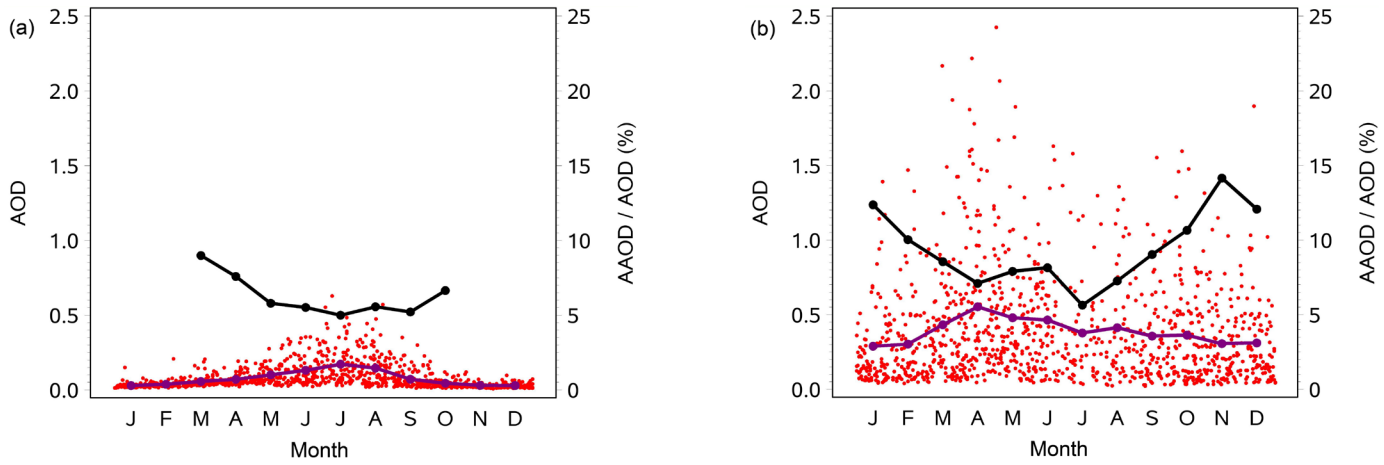

Figure 5-16. AERONET AOD and AAOD as a Percentage of AOD. (a) Goddard Space Flight Center (GSFC) in eastern United States and (b) Beijing, China from May 2005 to April 2009. Red dots represent AOD (shown on left vertical axis). Both AOD and AAOD are at 870nm. Horizontal axis shows the month of the year. The purple and black lines are the monthly average AOD and percent absorbing aerosol. Note that at GSFC, AOD is highest in the summer (associated with secondarily formed aerosols and winter-time AAOD observations are not available for GFSC because the calculation is not possible at low AOD values. (Source: AERONET data are based on Version 2, Level 2.0 inversion products with permission of Brent Holben, NASA and Hong-Bin Chen Chinese Academy of Sciences)

smaller for Europe and Southeast Asia, which are dominated by BC. The AERONET AAOD and OMI observations qualitatively agree with the ground level concentrations of BC for the United States, Europe, and Asia presented in Figure 5-14, and clearly increase the spatial characterization of aerosol absorption. As discussed below, aerosol absorption may not necessarily be associated with anthropogenic source emissions.

Multi-wavelength instruments, such as AERONET, can also characterize the wavelength dependence of absorption (often expressed as Absorption Angstrom Exponent, or AAE) to provide an indicator of the absorbing aerosol mixture. Using pairs of wavelength specific absorption measurements, Russell et al. (2010) find AAE values near 1 (the theoretical value for BC) for AERONET-measured aerosol columns dominated by urban-industrial aerosol, larger AAE values for biomass burning aerosols, and the largest AAE values for Sahara dust aerosols. Using these observations from multi-wavelength sensors can help distinguish the types of absorbing aerosols (Figure 5-14). It also demonstrates that the global AAOD observations presented in Figure 5-14 do not exclusively represent BC from anthropogenic sources.[17]

[17] The illustrative remote sensing observations presented in section 5.5 will be considerably strengthened when geostationary GLORY satellite with broad spectrum solar sensors to determine the global distribution of aerosol and cloud properties is deployed. Glory will provide 9-wavelength single-scattering albedo (SSA), AOD, AAOD, and AAE, as well as shape and other aerosol properties (Mishchenko et al., 2007; Russell et al., 2010).

While a common limitation of remote sensing (which depends on solar light) is its general representativeness of daytime and cloudless sky conditions, AAOD is additionally only representative of higher extinction periods required to make the needed absorption calculations. Consequently, AAOD for the United States and Europe is not based on measurements during the winter when atmospheric extinction is lower than the minimum computational threshold. Similarly, AAOD are not as well represented during the monsoon periods in Asia when AOD measurements are not available. These issues may be partially addressed by using seasonally or monthly weighted averages. Figure 5-15 illustrates the issue of incomplete data records and the contrast of AAOD levels across the globe.

Figure 5-16 presents AOD and AAOD as a percentage of AOD by date for two example locations from AERONET (Goddard Space Flight Center, GSFC in MD, and Beijing, China). The fraction of AOD that is estimated to be absorbing is lower at GSFC, but those data are not available during the winter months at GSFC due to insufficient AOD to calculate the absorbing portion. This is typical of the eastern United States and other U.S. locations where sufficient AOD only exists in the summer and which principally results from secondarily formed mostly scattering aerosols. Average percent absorbing aerosol for GSFC derived from AERONET is about 6-7%, but this does not represent winter-time conditions when BC may have its highest values.

In contrast, AOD is sufficiently high year-round in Beijing and is several times the amount detected at GSFC; the Beijing absorbing portion (black line) ranges from about 8-9% in the summer to 15% in the winter. For the 7 months of the year where both locations provide data, the ratio of monthly average AAOD values between Beijing and GSFC ranges from 2 to 7. However, without year-round AAOD data for GSFC, the estimate of its annual average absorbing aerosol and its annual average ratio to Beijing is very uncertain. Thus, the lack of wintertime absorption measurements limits the value of remote sensing estimates to expand the spatial extent of ground level measurements for model evaluation and corroboration of emissions inventories.

5.6 BC Observations from Surface Snow, Ice Cores, and Sediments

Snow and ice cover approximately 7.5-15% of the Earth's surface, depending upon the time of year (Kukla and Kukla, 1974). The sunlight that reaches the snow surface typically penetrates about 10-20 cm into the snow, with the topmost 5 cm receiving the most sunlight and where light-absorbing impurities can significantly alter the amount of solar energy reflected by the snowpack (e.g., Galbavy et al., 2007). Black carbon measurements in snow, and related surface reflectivity measurements, are critical to accurately estimate climate forcing due to snow-bound BC. In addition, ice core measurements of BC provide an important record of natural and anthropogenic BC emissions transported to snow-covered regions. Lake and marine sediments also pose an opportunity to derive historical trends in BC emissions prior to the point of time when air monitoring data are available.

5.6.1 Measurement Approach

Measurement of BC in snow or ice is a laborious process that begins with careful manual collection of snow or drilling an ice core. A sample of snow or ice is then melted and BC is quantified through several analytical approaches. The majority of researchers filter the melted snow or ice, collecting BC to the filter matrix and estimating BC by observing how light at certain wavelengths is absorbed by the particles (Grenfell et al., 1981; Clarke and Noone, 1985) or through a thermal or thermal-oxidative process (Ogren et al., 1983; Chylek et al., 1987). In addition, one newer approach avoids filtering the snow and quantifies BC by laser-induced incandescence (McConnell et al., 2007). The mass of the sample meltwater is measured and the final concentration units are usually in mass of BC per mass of snow or ice (e.g., ng BC/g snow).

Quantification of BC in sediments is an emerging field of study. The measurement technique is more complex than for snow or ice samples, as BC particles are embedded in sediment material that contains significant amounts of organic material. The sampling process usually involves extracting a sediment core and then slicing the core into layers. The BC particles are subsequently isolated for a given sample by applying a series of chemical and/or thermal treatments designed to remove non-BC material (Lim and Cachier, 1996; Kahn et al., 2009; Smith et al., 1973). Once the non-BC material is removed to the degree possible, BC concentrations are quantified via similar techniques utilized in ice core or ambient samples – measured by light absorption or through thermal processes. Microscopic analysis of carbon particles has also been employed to qualitatively determine the source type from the particle shape and surface texture (Kralovec et al., 2002; Smith et al., 1973).

5.6.2 Surface Snow Data

Measurements of BC in the shallow surface layer of snow have been conducted since the 1980s by research teams at locations throughout the Northern Hemisphere and in Antarctica, although the measurements were sporadic (Figure 5-17). Two large field studies, Clarke and Noone (1985) and Doherty et al. (2010), significantly boosted the number of sampling locations during two windows of time (1983-1984, 2006-2009). However, even the highest number of measurement locations (55 sites in 2009) provides sparse geographic coverage of data, considering the high degree of spatial variability in BC concentrations. Recent model estimates by Flanner et al. (2007), seek to fill in the missing measurement gap with predictions of surface snow BC concentrations in the northern hemisphere, estimating values ranging five orders of magnitude (<1 to >1000 ng BC/g snow).

Recent surface snow results from Doherty et al., (2010) show that BC concentrations range over an order of magnitude in remote areas of the Northern Hemisphere (Figure 5-18). Even higher BC values in snow were reported for the Tibetan Plateau and throughout western China, up nearly another order of magnitude (Ming et al., 2009; Xu et al., 2006). BC removal from the atmosphere is primarily driven by precipitation (Ogren et al., 1984), thus BC concentrations in snow or ice are a function of the atmospheric concentration of BC above the surface and the frequency and amount of snowfall in a particular area. For example, Xu et al. (2009b) noted that BC concentrations on the Tibetan plateau were high during nonmonsoon periods with low precipitation, which they related to regional

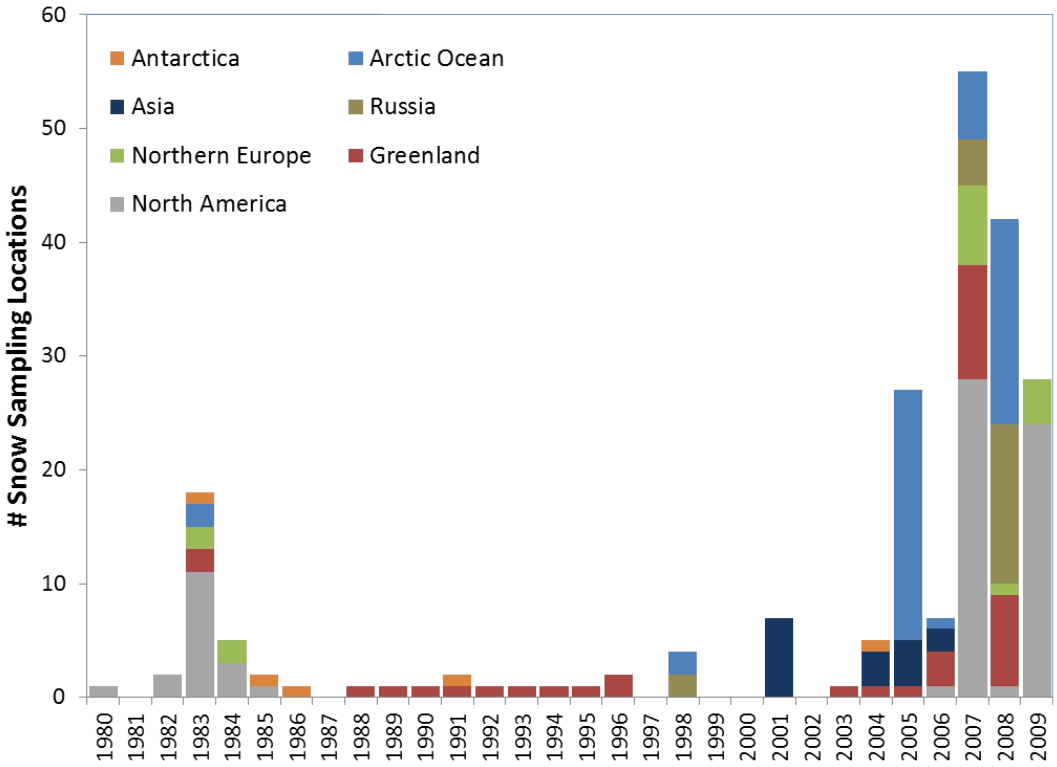

Figure 5-17. Locations of BC Measurements in Surface Snow and Shallow Snow Pits (snow pits are indicated for each year covered in the pit depth). (Sources: U.S. EPA, based on data reported in Cachier and Pertuisot (1994), Cachier (1997), Chylek et al. (1999; 1987), Clarke and Noone (1985), Doherty et al. (2010), Grenfell et al. (2002; 1981; 1994), Hagler et al. (2007a; 2007b), Hegg et al. (2009; 2010), Masclet (2000), Ming et al. (2009), Perovich et al. (2009), Slater et al. (2002), Warren and Clarke (1990), Warren et al. (2006), and Xu et al. (2006))

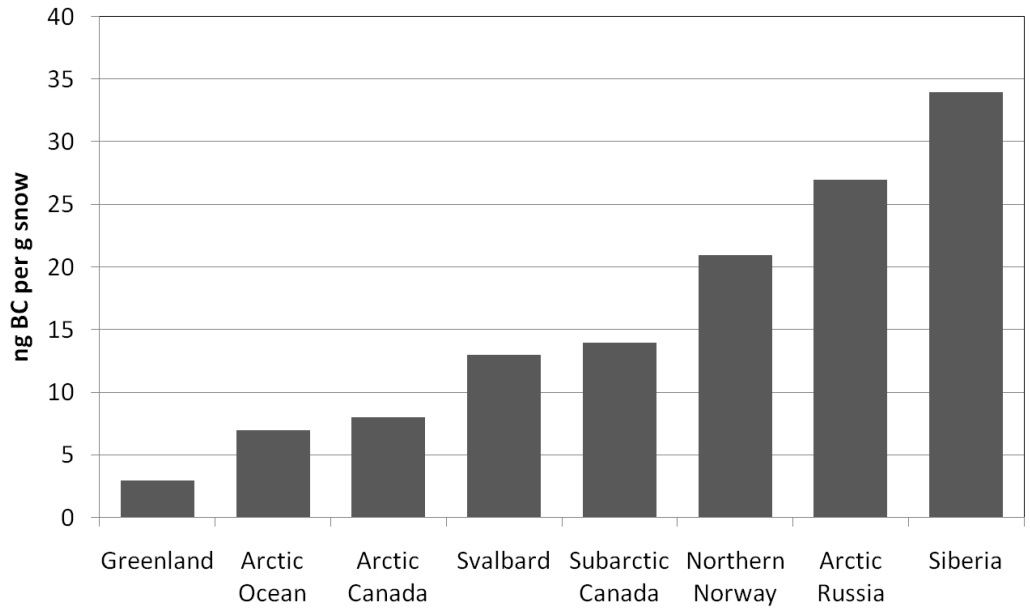

Figure 5-18. BC Concentrations in Surface Snow in Arctic and Subarctic Areas of the Northern Hemisphere. (Source: Derived from recent measurements reported in Doherty et al., 2010)

particulate pollution ("Asian Brown Cloud") elevating during the dry nonmonsoon period and then highly concentrating the infrequent precipitation with impurities. An additional important factor, discussed by several studies (Doherty et al., 2010; Flanner et al., 2007; Grenfell et al., 2002; Xu et al., 2006) is the potential increase in surface snow BC levels when melting snow leaves behind BC particles, further darkening the topmost layer of snow.

It is important to note that certain non-BC particulate species have been shown to absorb light when deposited to snow or ice. While dust is not as strong of a light absorber per unit mass as BC, dust can play a significant role in reducing snowpack reflectivity at high concentrations (Warren and Wiscombe, 1980). In addition, BrC in snow has been suggested to significantly absorb light (Doherty et al., 2010). Given that studies suggest that organic material in snow may undergo chemical transformation and loss from the snowpack due to sunlight-driven reactions (Hagler et al., 2007a; Grannas et al., 2004), BrC may absorb light to an even greater degree in fresh precipitation than what has been measured in aged snow samples. However, neither Grannas et al. nor Hagler et al. specifically measured BrC or the time evolution of light absorption.

5.6.3 Ice Core Data

Measurements of BC in ice cores are critical to understanding the longer-term trends of human influence on snow reflectivity. Ice cores, produced by drilling into permanent ice and carefully extracting a column of ice, have been collected and analyzed for BC at a number of locations in the Northern Hemisphere (Figure 5-19). In addition, an Antarctic BC ice core record spanning the past two and a half thousand years has just been completed as part the National Science Foundation WAIS Divide deep ice core project (Ross Edwards, personal communication). The ice cores with continuous BC data available primarily cover the past few hundred years, with the exception of the Dye 3 ice core in Greenland and the WAIS Divide core in Antarctica which extend back several thousand years. The layers of the ice core are dated using several strategies, including measuring certain chemical species with known seasonal variation, looking for certain known historical events that had unique

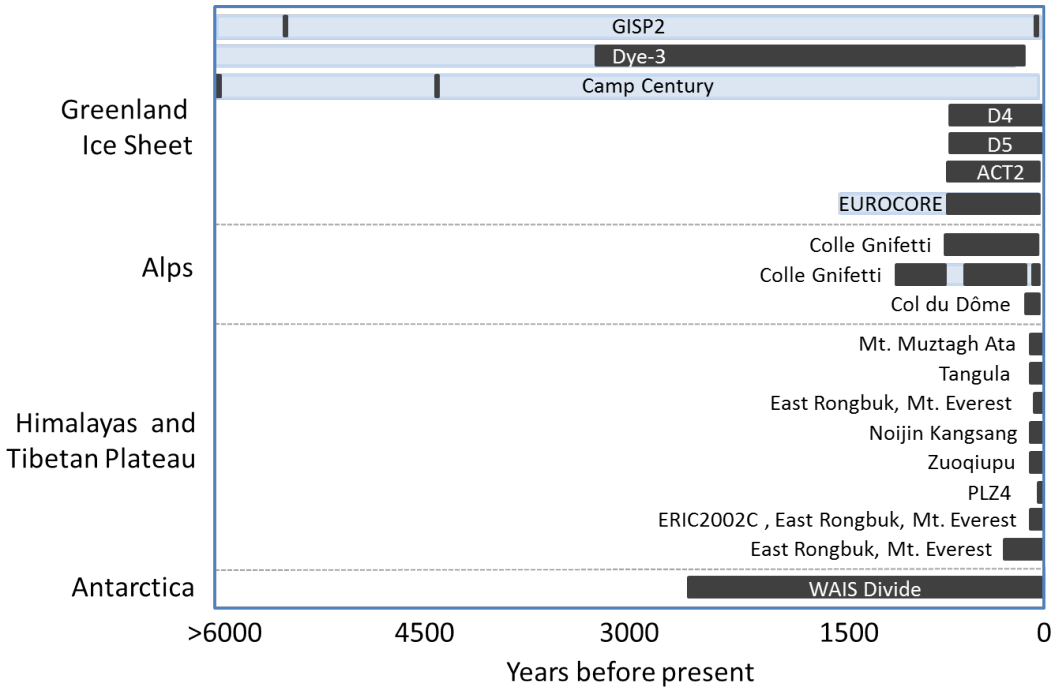

Figure 5-19. BC Ice Core Records Worldwide Labeled by Their Identifying Name. The extent of the bars (light blue and/or black) shows the time covered by the depth of the ice cores, with the black regions representing sections of the ice core that had BC concentrations reported. (Source: U.S. EPA, based on data reported in Cachier and Pertuisot (1994), Chylek et al. (1987; 1992; 1995), Ross Edwards (personal communication regarding WAIS Divide ice core), Kaspari et al. (2011), Lavanchy et al. (1999), Legrand et al. (2007), Liu et al. (2008b), McConnell et al. (2007), McConnell and Edwards (2008), Ming et al. (2008), Thevenon et al. (2009), and Xu et al. (2009a; 2009b))

chemical signatures (e.g., volcanic eruptions, nuclear explosions), and observing the visible layering of ice throughout the core (e.g., Hammer, 1978).

The concentrations of BC in a certain ice core reflect the past atmospheric concentrations above the region, which in turn relate to short- and long-distance transport of BC emissions. Thus, the ice core results vary from location to location. For example, on the remote Greenland Ice Sheet, McConnell (2010) showed a peak in BC concentrations in the 1910-1920 time range, decreasing in concentration from that point to present day. Meanwhile, ice cores in the European Alps show BC concentrations increasing significantly past the 1910-1920 period, with highest concentrations recorded in the 1950-1960 time frame (Lavanchy et al., 1999; Legrand et al., 2007). Finally, Xu et al. (2009b) and Ming et al. (2008) reveal variable results for multiple shallow ice cores collected in the Himalayas and Tibetan Plateau that date from the 1950s to 2004: several ice cores have highest BC levels in the 1960s and lower levels from that point forward, while another ice core had continuously increasing levels until present day. Studies of ice core data collected to date find associations between elevated BC and human activities; however, the trends vary significantly by location.

5.6.4 Sediment Data

With ice core records only available in remote, high-altitude locations in the world, undisturbed lake sediments provide additional spatial coverage of BC historical trends and may demonstrate higher associations with local emissions. In addition, deep ocean marine sediments reveal ancient BC trends related to natural emissions. Similar to ice cores, BC records in sediments initiate from the deposition of BC from the atmosphere, which relates to the atmospheric transport of BC emissions to a particular location. After depositing to the surface of a water body, the BC particles eventually transport downwards and, if the sediment is undisturbed, may form a permanent archive in the layers of sediment.

Lake sediment BC records have been quantified for several interior lakes in North America, including Lake Michigan, dating 1827-1978 (Griffin and Goldberg, 1983), and four lakes located in the Adirondacks of New York, dating 1835-2005 (Husain et al., 2008). Total carbon particles, associated with specific sources by particle shape, have also been measured in Lake Erie sediments, dating 1850-1998 (Kralovec et al., 2002). Historical BC records have also been obtained for a number of lakes in the Alps of northern Slovenia (Muri et al., 2002; 2003) and in ancient marine sediments, aged approximately 100 million to 5000 years before present, spanning southern to far northern latitudes of the Pacific Ocean and at several locations in the Atlantic Ocean (Smith et al., 1973).

The findings by Smith et al. (1973) reveal an approximate 10-fold increase in ancient BC deposited levels moving from the equator northward to 60°N (bisecting Canada), which they related to the increase in natural wildfire emissions moving from the equator northward. These trends lay the base pattern of deposited BC, to which anthropogenic emissions of BC would be added. Focusing on sediment findings that closely relate to U.S. emissions, Figure 5-20 presents estimates of atmospheric BC derived from sediment core measurements in the Adirondack region of New York State for deposition from approximately 1835 to 2005 (Husain et al., 2008) and overlays these estimates with long-term U.S. BC emissions data developed by Novakov (2003). The derived BC ambient estimates are well correlated with the historical BC emissions estimates for fossil fuel combustion in the United States, and Husain et al. (2008) attributed the decrease from 1920-2000 to reduction in BC emissions from U.S. fossil fuel combustion.

The ambient BC determined from Adirondack lake sediments by Husain et al. (2008), shown above, can be compared with records obtained from Lake Michigan sediments from Griffin and Goldberg

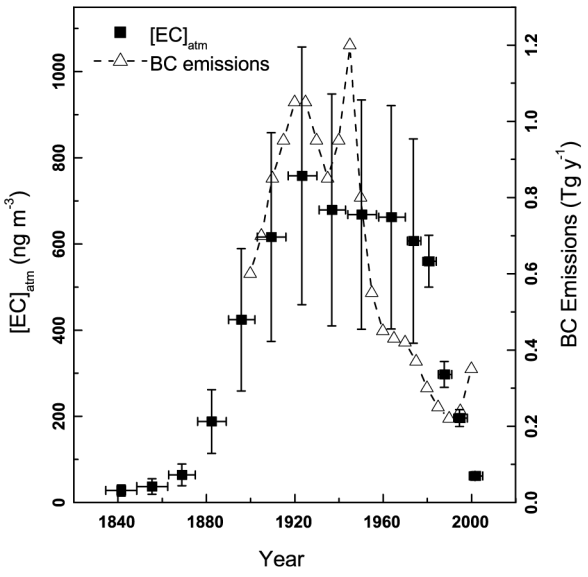

Figure 5-20. Atmospheric BC determined by Husain et al. (2008), for the Adirondack Region from 1835 to 2005. The measurements are compared with U.S. BC emissions. (Novakov et al., 2003)

(1983) and from Lake Erie sediments (Kralovec et al., 2002). While the multiple archives in multiple North American lake sediments reveal a significant increase in deposited BC levels after the late 1800s, the Lake Michigan time series shows an apparent peak in the record around 1940-1960, while the Adirondacks show a peak near 1910-1930, and the Lake Erie record shows a peak in 1970-1980. It is uncertain why the multiple sediment records in North America contrast in the timing of the peak BC concentration; possible explanations may include differences in local versus regional source contributions, dating methodology, carbon measurement approaches, and sediment deposition processes.

5.6.5 Arctic BC Snow and Ice Data – Source Identification

Impacts of BC emissions on the Arctic are of particular interest given the climate-sensitive nature of the region. BC emissions from particular source types or regions and transport to the Arctic have been explored through modeling studies and field measurements. This section discusses the findings in observational BC data from Arctic snow and ice. Connections between snow and ice BC data and source types are generally made by measuring additional species in the snow (i.e., ions, metals, organics, and isotopes) and comparing trends between the multiple data sets.

Historical trends in Arctic ice cores collected on the Greenland Ice Sheet improve our understanding of the historical impact of anthropogenic and natural emissions of BC on the Arctic. McConnell and Edwards (2008) and McConnell et al. (2007) provide monthly-resolution BC data in ice cores on the Greenland Ice Sheet. Similar to the lake sediment findings for the Adirondack Mountain region, the maximum BC concentrations in Arctic ice in the past hundred years occurred in the early 1900s corresponding to increases in a number of species associated with industrial emissions (e.g., cadmium, cesium, thallium, lead). McConnell et al. (2007) compare vanillic acid (VA), non-sea-salt sulfur (nss-S), and BC trends to apportion the BC due to industrial versus forest fire emissions (see Figure 5-21). VA is considered an indicator of forest fire emissions, while nss-S relates to industrial emissions and volcanic eruptions. In the postindustrial era, BC anthropogenic emissions contributed roughly 50-80% of the total BC loading in the ice during early 1900s and over past few decades the industrial input was on the order of 20-50% (estimated from Figure 5-21, originally published in McConnell et al., 2007). While nss-S correlated highly with the increasing BC during the late 1800s to mid-1900s, the trends did not match later; this may be related to changes in industrial emission factors. This study associates the high BC concentrations in the early 1900s with North American fossil fuel emissions and suggests that Asian emissions may play an important role past the mid-1900s.

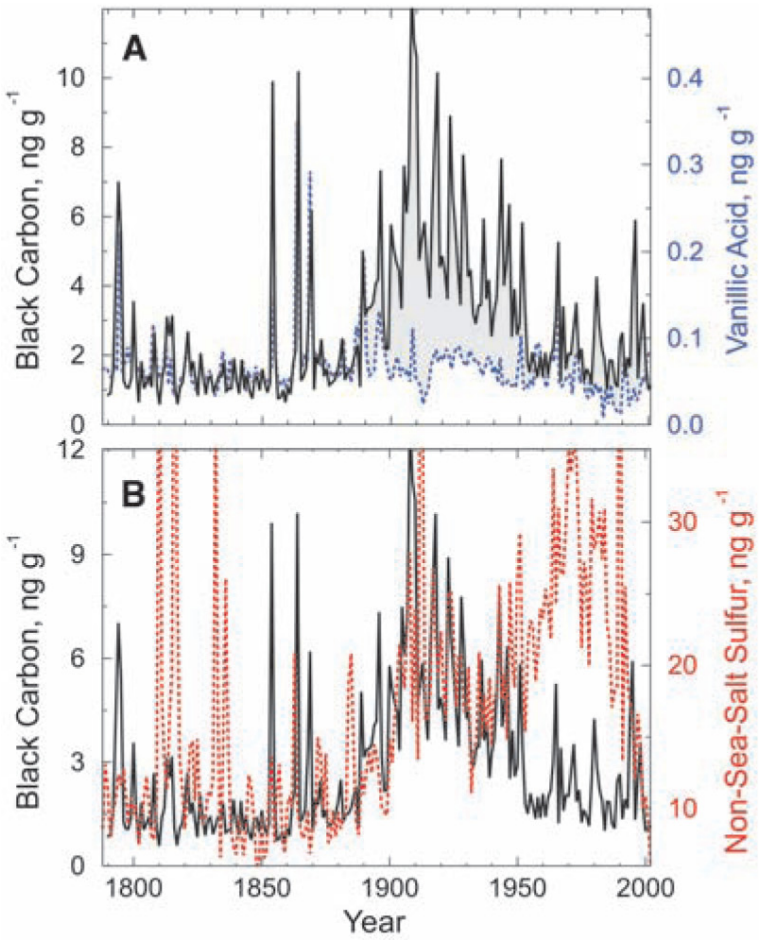

Figure 5-21. Annual Average Concentrations of (a) BC and VA and (b) BC and Non-Sea-Salt Sulfur (nss-S). The gray shaded region (between the black and blue dotted line) in the top figure represents the portion of BC attributed to industrial emissions, not boreal forest fires. (Source: Adapted from McConnell et al. (2007))

Two recent studies attempted to attribute BC in snow to specific sources by collecting a large number of surface snow samples throughout the Arctic, which they measured for detailed chemical composition (Hegg et al., 2009; 2010). In Hegg et al. (2010), statistical analyses revealed that the measured species could be grouped into four unique factors with source-defining chemical characteristics (for example, sodium and chloride indicating a marine environment), which the authors labeled as marine, boreal biomass, crop and grass biomass, and pollution. It should be emphasized that the "marine" category represents air masses with an ocean-like chemical signature (i.e., sea salt), which may also include emissions from other sources (biomass or fossil fuel combustion) that transported over the ocean and mixed with sea spray. Depending on the location of the sample within the Arctic and time of year, the estimated contribution from these four sources varied considerably (Figure 5-22). In Siberia, emissions from biomass burning were significant drivers of BC and other absorbing species. However, on the Greenland Ice Sheet and at the North Pole, pollution and crop/grass biomass were found to be the primary sources.

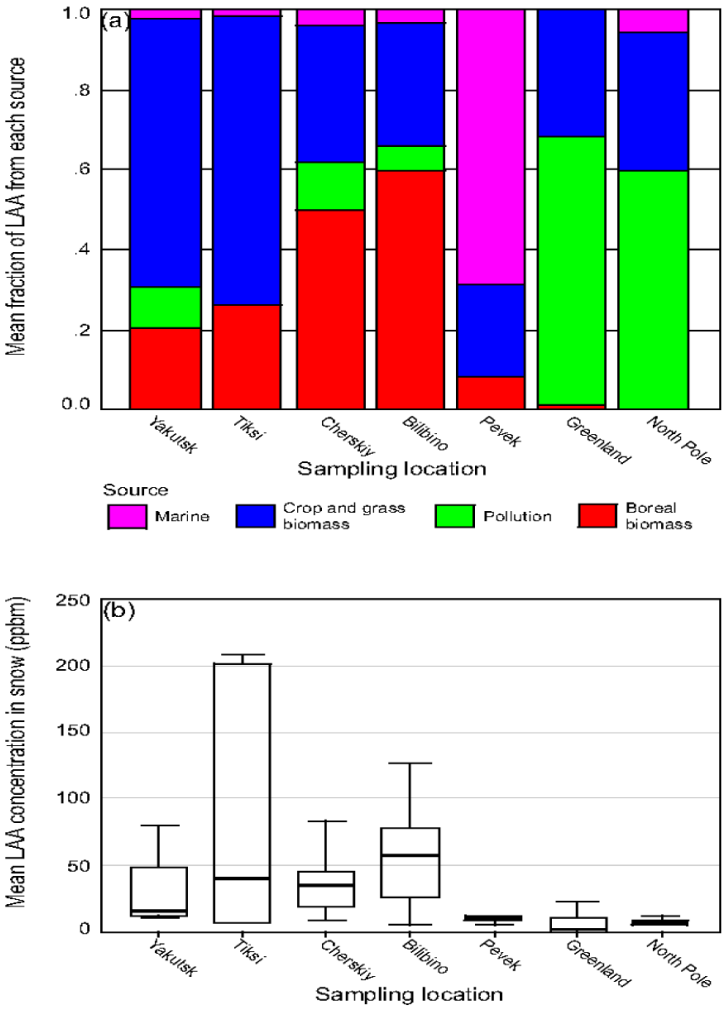

Figure 5-22. Sources of BC in Arctic Snow. (a) Fractional source contributions to Light Absorbing Aerosol (LAA) snow concentrations in Siberia (Pevek, Billbino, Cherskiy, Tiksi, Yakutsk), the Greenland Ice Sheet, and the North Pole. (b) The box and stem plots represent concentrations of LAA at each location, with error bars indicating the 95% confidence interval. LAA values are derived from a light absorption technique which converts to a mass estimate using calibration factors and are generally equivalent to BC values, although non-BC absorbing aerosols could bias the estimate high. (Source: Hegg et al., 2010)

5.7 Limitations and Gaps in Current Ambient Data and Monitoring Networks

The primary limitation in existing ambient monitoring data is the sparse geographic coverage of existing BC monitoring locations. There are parts of the world where there currently are no measurements; and where they do exist, the measurements are not archived into a consolidated database. The differences in average BC concentrations between countries (global scale), among regions (regional scale) and also within cities (local scale) are all much larger than the differences across monitoring methods. These geographic variations are also larger than the inter-annual changes that may occur within a 5-to-10-year period. To help develop and corroborate emissions inventories and to evaluate global models (see Chapters 4 and 2, respectively), additional ambient measurements are needed at more locations. Existing geographically dense filters used to produce $PM_{2.5}$ measurements in the United States (and elsewhere if available) can be used to cost-effectively supplement the measurements from more specific and expensive BC monitors. Also currently there are insufficient measurements characterizing the BrC component of OC. The addition of more multiple wavelength optical analyzers or use of optical measurements from existing $PM_{2.5}$ filter samples would be useful (Hecobian et al., 2010; Chow et al., 2010b).